

CHAPTER IV

MATHEMATICAL MODEL

In simulating crude oil distillation systems, the conventional empirical methods are replaced by rigorous calculations using computer models. In the present work two models, one for crude oil and one for topping column, have been developed for process simulation. This chapter describes the basic features of these models, their use in simulation, and their possible use to improve refinery operations.

4.1 Crude Oil and Petroleum Fraction Models

Crude oil and petroleum fractions, being composed of such a large number of hydrocarbon compounds that it is not feasible to identify them or to determine the composition in terms of pure components, may be described as complex mixtures. Because these mixtures cannot reasonably be represented by a series of true components having specific compound properties, it is necessary to characterize them in some indirect manner using empirically determined average properties.

Generally, the principal method used is based upon the pseudomulticomponent concept. This method is not new. In fact, Katz and Brown (50) described the method in 1933. Further discussions of the method were made by Edmister (43) and Poettman and Mayland (51). In this method the mixture is considered to be composed of a number

of cuts or portions, each of which can be characterized with an average boiling point, an average density, an average molecular weight, and an average molecular characterization. With such properties estimated for each of the cuts or portions and with availability of some further correlation of vapor-liquid equilibrium concentrations as a function of temperature and pressure, the multicomponent distillation method, which will be discussed later can be applied to the crude oil for simulation.

No method, including the pseudomulticomponent method, is exact because of the assumptions necessary to assign average properties to each of the pseudocomponents and to reduce the complexity of the calculations, and because of the generalized nature of the correlations (32). However, with digital computers, the pseudomulticomponent method becomes more practical. The necessary average properties of the pseudocomponents can be obtained by the following procedures.

4.1.1 Number and Quantities of Components

The approach adopted here is to divide the crude oil, or petroleum fraction, TBP curve into pseudocomponents and then handle them as pure components in the calculations. For practical calculations, the number of hypothetical pseudocomponents into which the TBP curve should be divided depends upon the accuracy desired. However, the width of these hypothetical pseudocomponents should not exceed 5-7 volume percent (31). The components are obtained by means of the chord area method shown in Fig.13. The shaded areas on both sides of the curve should be equal. Each of the hypothetical pseudocomponents

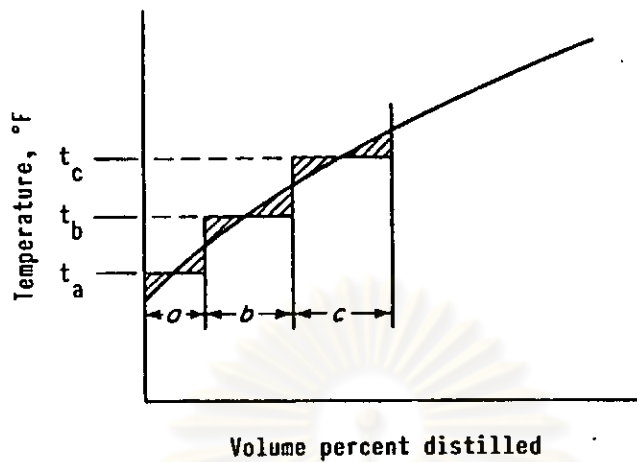


Fig.13 Breakup of TBP distillation curve into pseudocomponents.

is identified by its average boiling point on the TBP curve. The volume percent of each component is then obtained from the figure. These volume percent increments, which represent the pseudocomponent properties and also include volume percent of each actual component or light hydrocarbon in the mixture, are converted to weight and then to moles. With the moles of each component, suitable vapor-liquid equilibrium ratios, and vapor/liquid enthalpies, the column calculations can be proceeded.

4.1.2 Density and Specific Gravity

With crude assay, or crude oil for which laboratory crude analyses are available, curves of specific gravity vs. volume percent recovered on a TBP distillation usually are available. In these cases, the gravity corresponding to the mid-volume of each pseudocomponent is used as data.

In many cases of petroleum fractions, a gravity-volume percent curve is not available, but the gravity of the entire

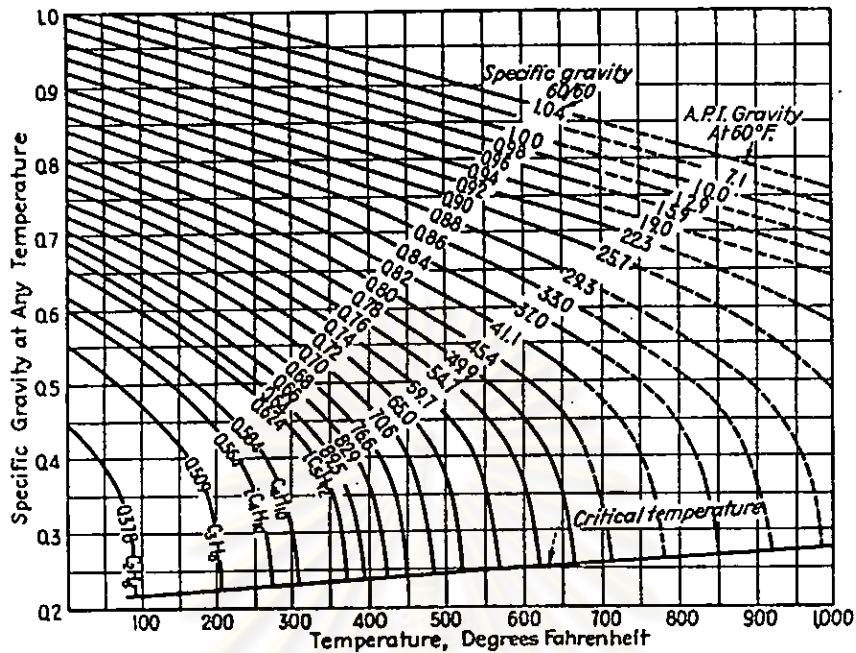


Fig.14 Approximate change of specific gravity of intermediate-base oils with temperature (4).

fraction is known. This, plus an ASTM distillation curve of fraction, permits calculation of the UOP characterization factor (UOP-K). In these cases, it is assumed that each pseudocomponent will have the same characterization factor so that the gravity of each pseudocomponent is calculated by (4)

$$\text{Sp.Gr.}(60/60^{\circ}\text{F}) = \sqrt[3]{T_B} / (\text{UOP-K}) \quad (10)$$

where T_B = average boiling point (ABP) temperature, °R.

Density is defined as weight per unit volume. In the petroleum industry, density is usually expressed as pounds per gallon. Since 1 gal of water at 60°F weights 8.328 lb, the density is

$$\text{Density, lb/gal} = \text{Sp.Gr.} \times 8.328 \quad (11)$$

The relation among API gravity, specific gravity, and density (52) is given in the tables in Appendix A.

The approximate density of petroleum fractions at elevated temperatures (4) can be obtained from Fig.14. The figure relates the specific gravity at 60°F with the specific gravity at other temperatures. The number accompanying each line indicates the gravity of the material at 60°F.

4.1.3 Molecular Weight

Correlation of molecular weight with specific gravity and boiling point is based on a curve presented by Smith (53), which shows the relation between reciprocal absolute boiling point and specific gravity for various homologous series. Smith's work was primarily concerned with obtaining a constitution index for crude oil fractions. The relation of this graph to molecular weight, however, is quite clear.

Watson (54) presented a correlation of boiling point and density with molecular weight as shown in Fig.15, but the derivation and statistical evaluation were not given. The boiling point-density correlation developed by Mills and coworkers (55) was, for the most part, in close agreement with that of Watson and based on true boiling points. An average deviation of 2.4 percent for ordinary range of petroleum fractions (about 70 - 300 molecular weight) was reported.

Winn (56) correlated many of the properties of petroleum

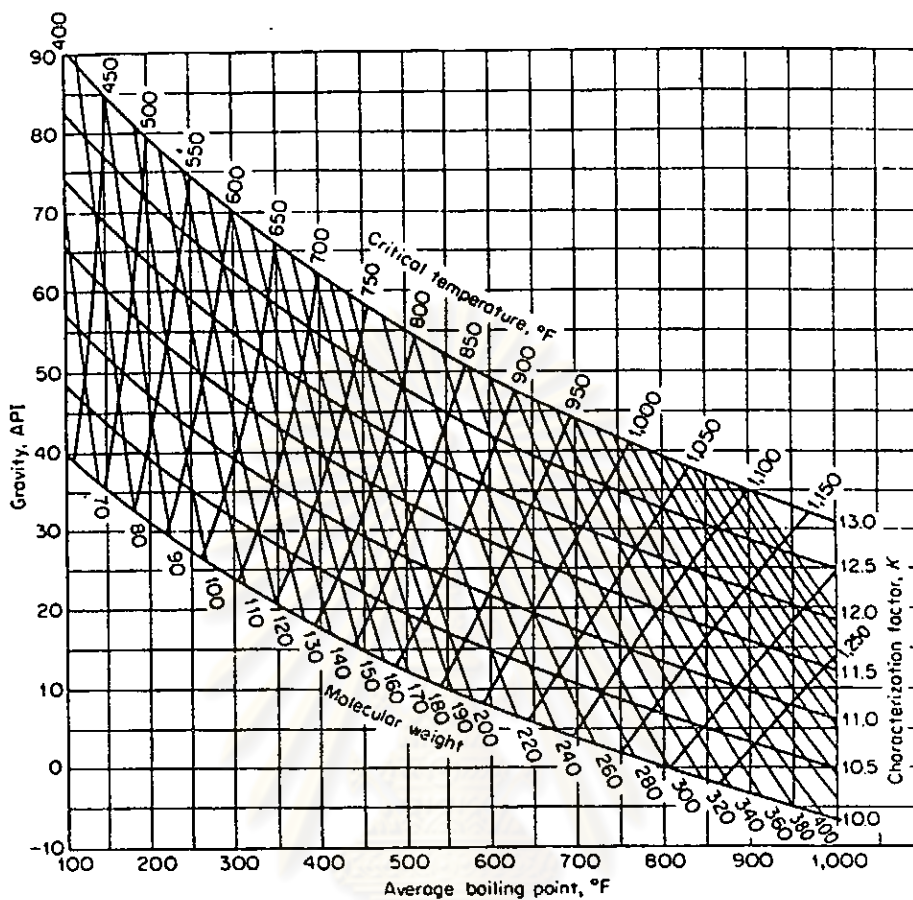


Fig. 15 Molecular weights, critical temperatures, and characterization factors of petroleum fractions (54).

fractions including the average molecular weight by the use of nomogram as shown in Fig. 17. The experimental average molecular weight data of several petroleum fractions that have been determined by Fenske and McCluer (57), FitzSimons and Thiele (58), Mills et al. (55) and certain other researchers indicate that the average deviation is about 3 percent from nomographic values.

Hariu and Sage (38) derived an essential equation by a surface-fit of the Winn nomograph, which extends to 600 molecular weight and 1200°F normal boiling point. The equation was extrapo-

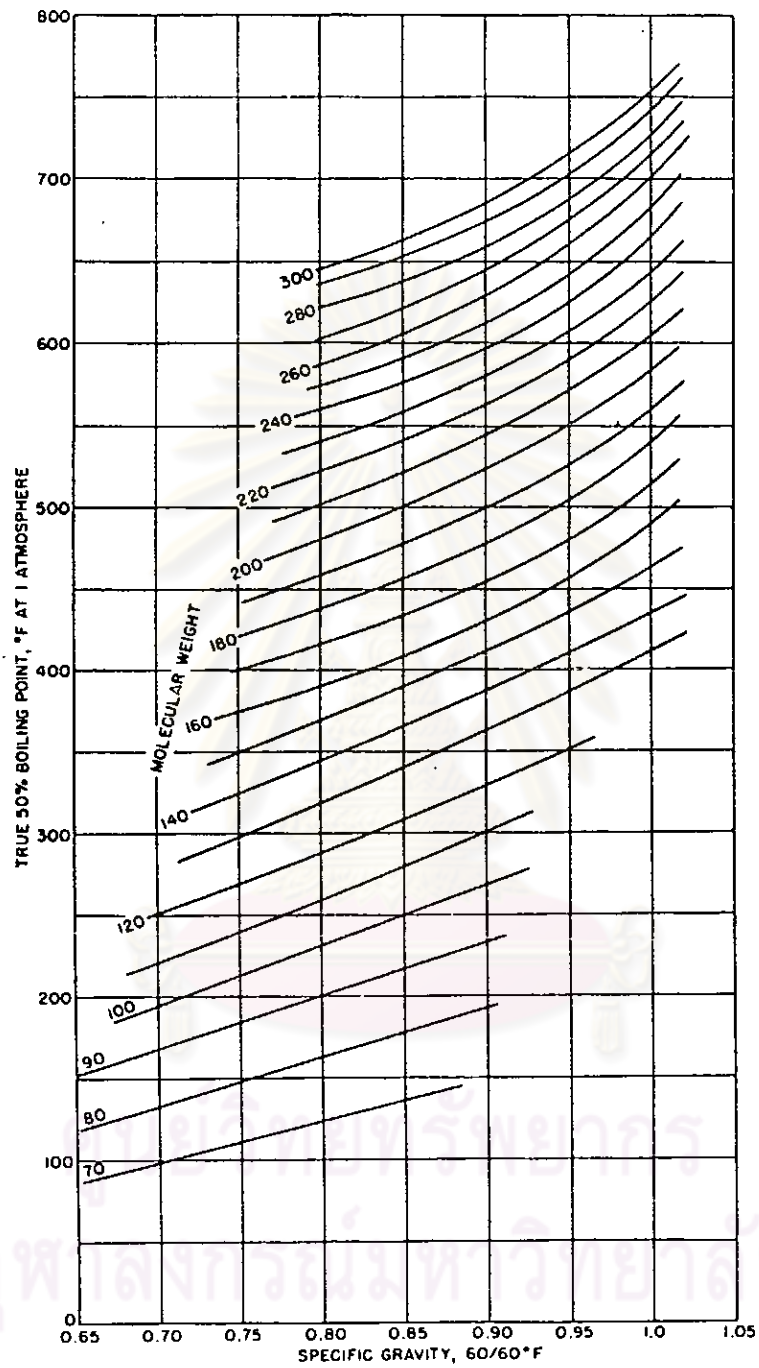


Fig.16 Molecular weights on true 50% boiling point versus gravities of petroleum fractions (55).

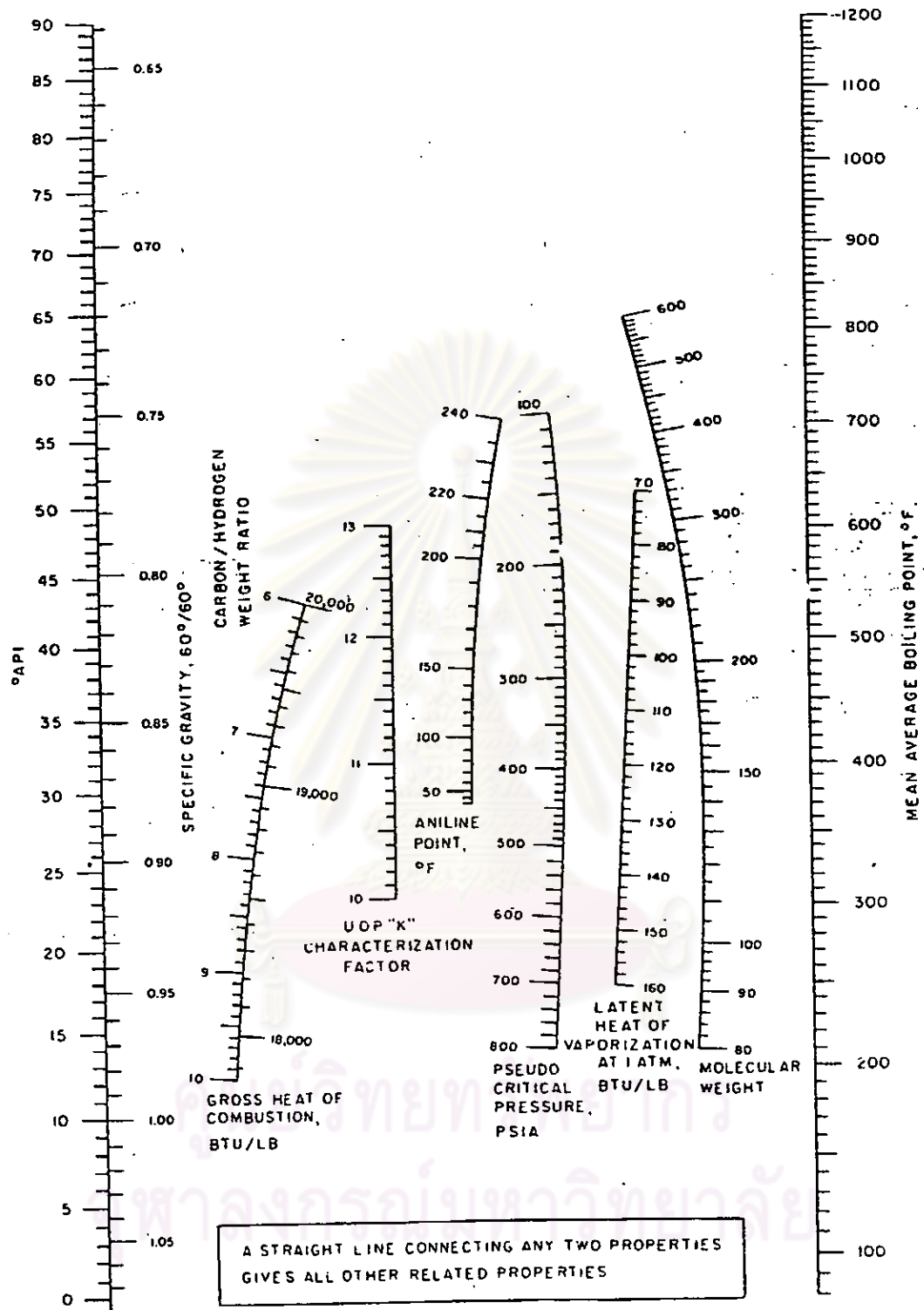


Fig.17 Winn's Nomograph - Related properties of petroleum fractions (56)

lated to over 1500°F normal boiling point by including in the surface fit input estimated boiling points and gravities of very high molecular weight hydrocarbons, but the accuracy of this equation was not reported. The molecular weight equation is

$$\log_{10}(\text{MW}) = \sum_{i=0}^2 \sum_{j=0}^2 A_{ij} X^i Y^j \quad (12)$$

where X = Average boiling point, °F

Y = UOP Characterization Factor

and $A_{00} = +0.6670202$

$A_{10} = +4.583705 \times 10^{-3}$

$A_{20} = -2.698693 \times 10^{-6}$

$A_{01} = +0.1552531$

$A_{11} = -5.755585 \times 10^{-4}$

$A_{21} = +3.875950 \times 10^{-7}$

$A_{02} = -5.378496 \times 10^{-3}$

$A_{12} = +2.500584 \times 10^{-5}$

$A_{22} = -1.566228 \times 10^{-8}$

Maxwell (44) derived a molecular weight chart for petroleum fractions, as shown in Fig.18, from an empirical correlation of molecular weight and the function, $T_B/\text{Sp.Gr.}^{0.40}$, where T_B is the average boiling point of the fraction in °R, and Sp.Gr., the specific gravity at 60/60 °F. The average deviation for about one hundred petroleum fractions of 75 - 500 molecular weight is 2 percent. An equation having an average deviation of less than one percent from the chart is developed in the present work to fit this chart, i.e.

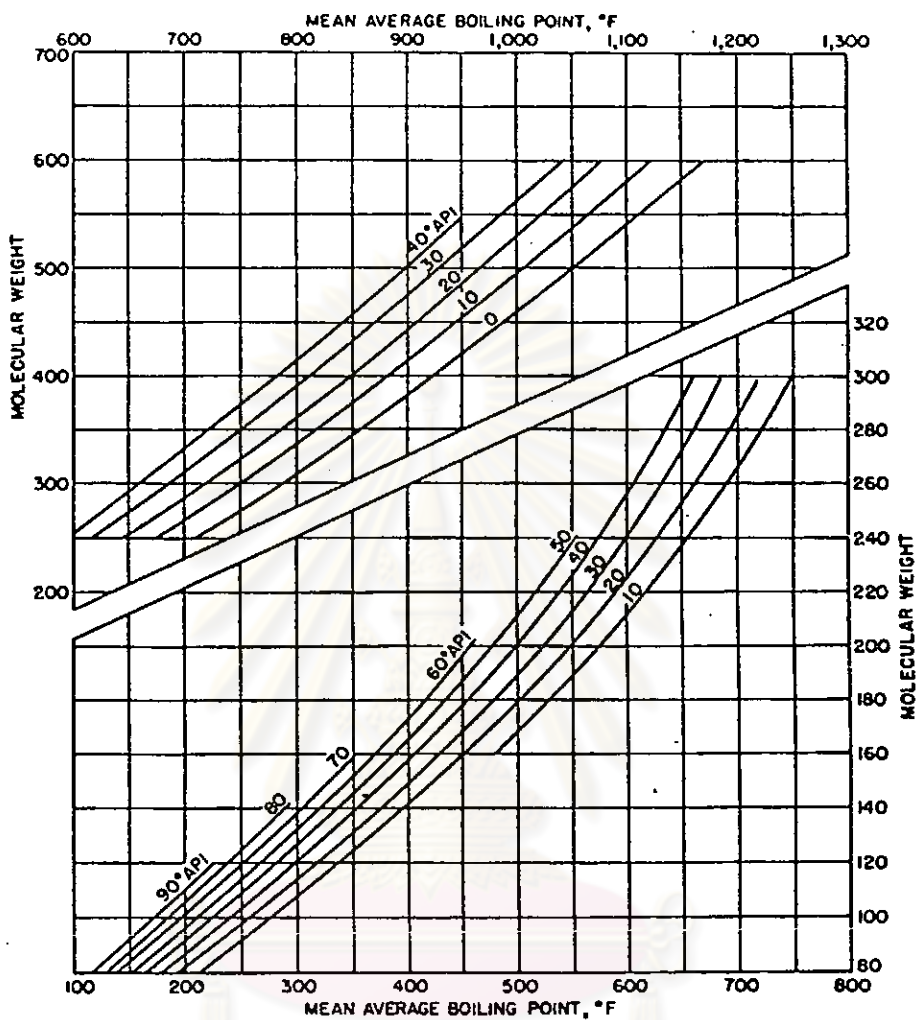


Fig.18 Molecular weights versus boiling points of petroleum fractions (44)

$$MW = \sum_{i=0}^2 \sum_{j=0}^2 B_{ij} X^i Y^j \quad (13)$$

where X = Average boiling point, °F

Y = API Gravity

and $B_{00} = +3.63011$

$B_{10} = +3.323389 \times 10^{-3}$

$B_{20} = -8.700594 \times 10^{-7}$

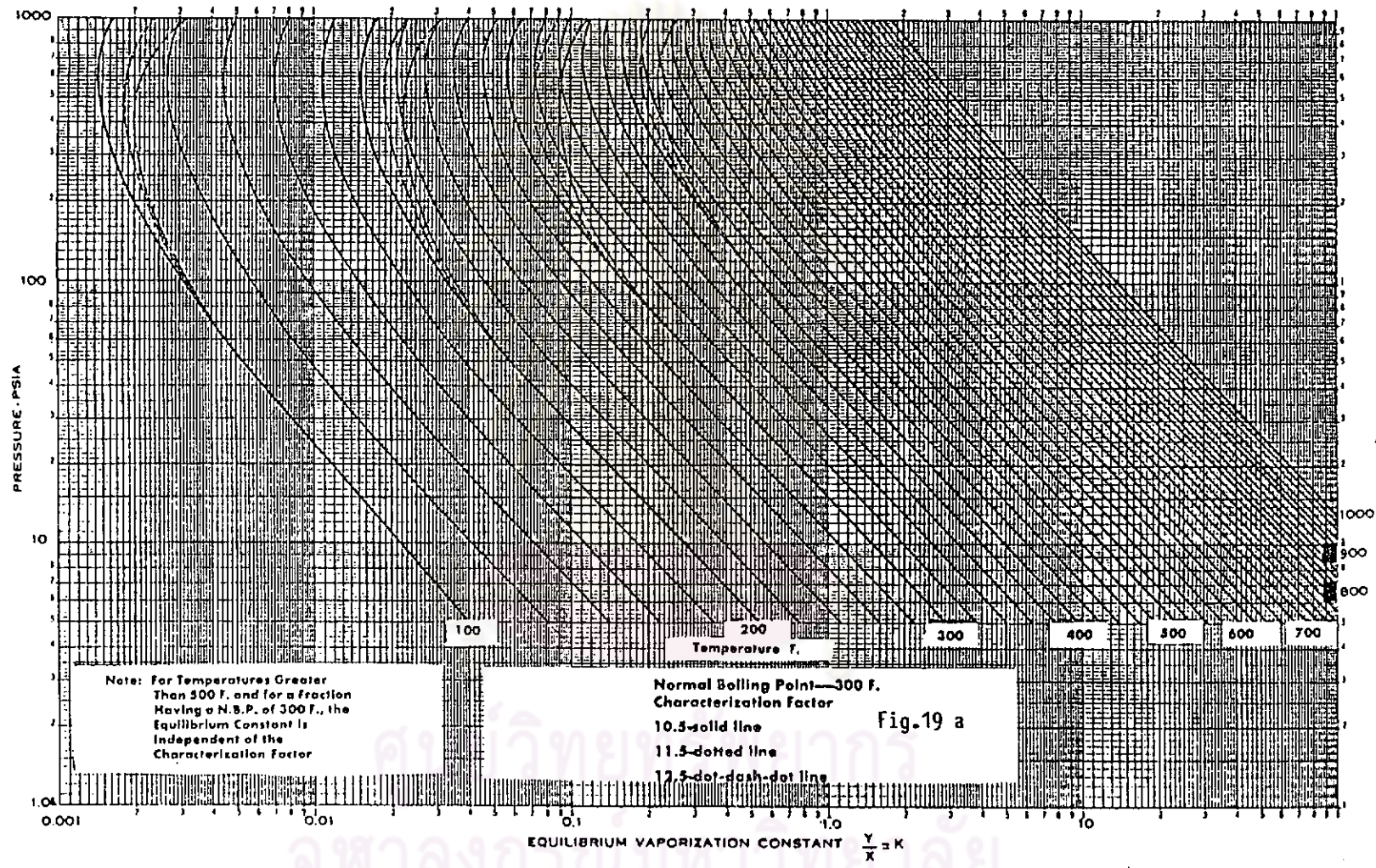
$$\begin{aligned}
 B_{01} &= +5.870290 \times 10^{-3} \\
 B_{11} &= +4.254180 \times 10^{-9} \\
 B_{21} &= -2.546188 \times 10^{-5} \\
 B_{02} &= -1.007117 \times 10^{-6} \\
 B_{12} &= +9.442635 \times 10^{-8} \\
 B_{22} &= -1.251384 \times 10^{-10}
 \end{aligned}$$

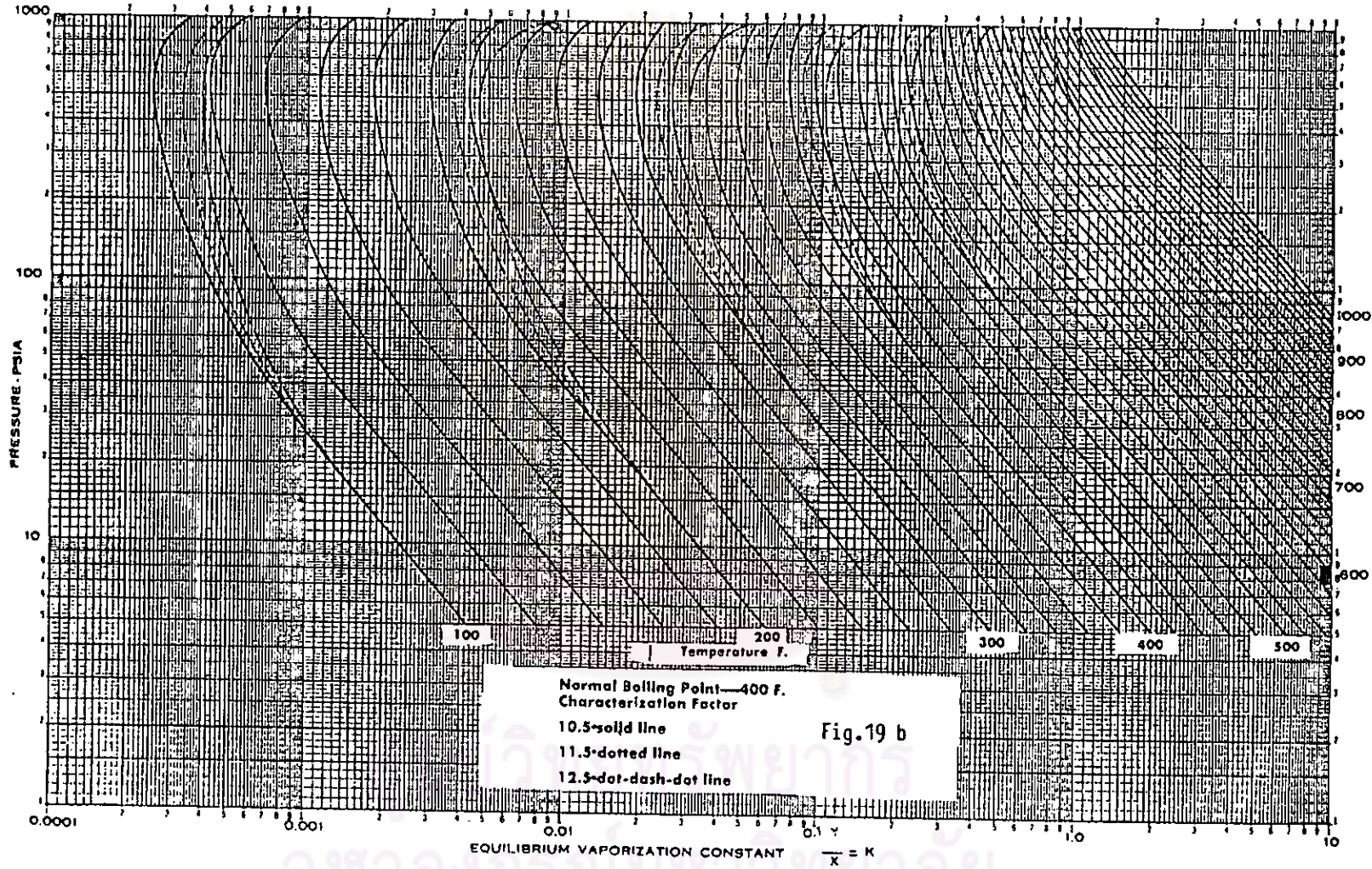
4.1.4 Vapor-Liquid Equilibrium, K-values

One most important property of pseudocomponents, of course, is the vapor-liquid equilibrium ratio or K-value. Several authors have published curves or correlations giving K-values as functions of temperature, pressure and average boiling point. Poettman and Mayland's curves (51), as illustrated in Fig.19a-h, go up to 1,000°F NBP but are of questionable accuracy because they are based on Cox chart vapor pressures, which are not reliable for high boiling point fractions (38). None of the others cover petroleum fractions boiling over 800°F.

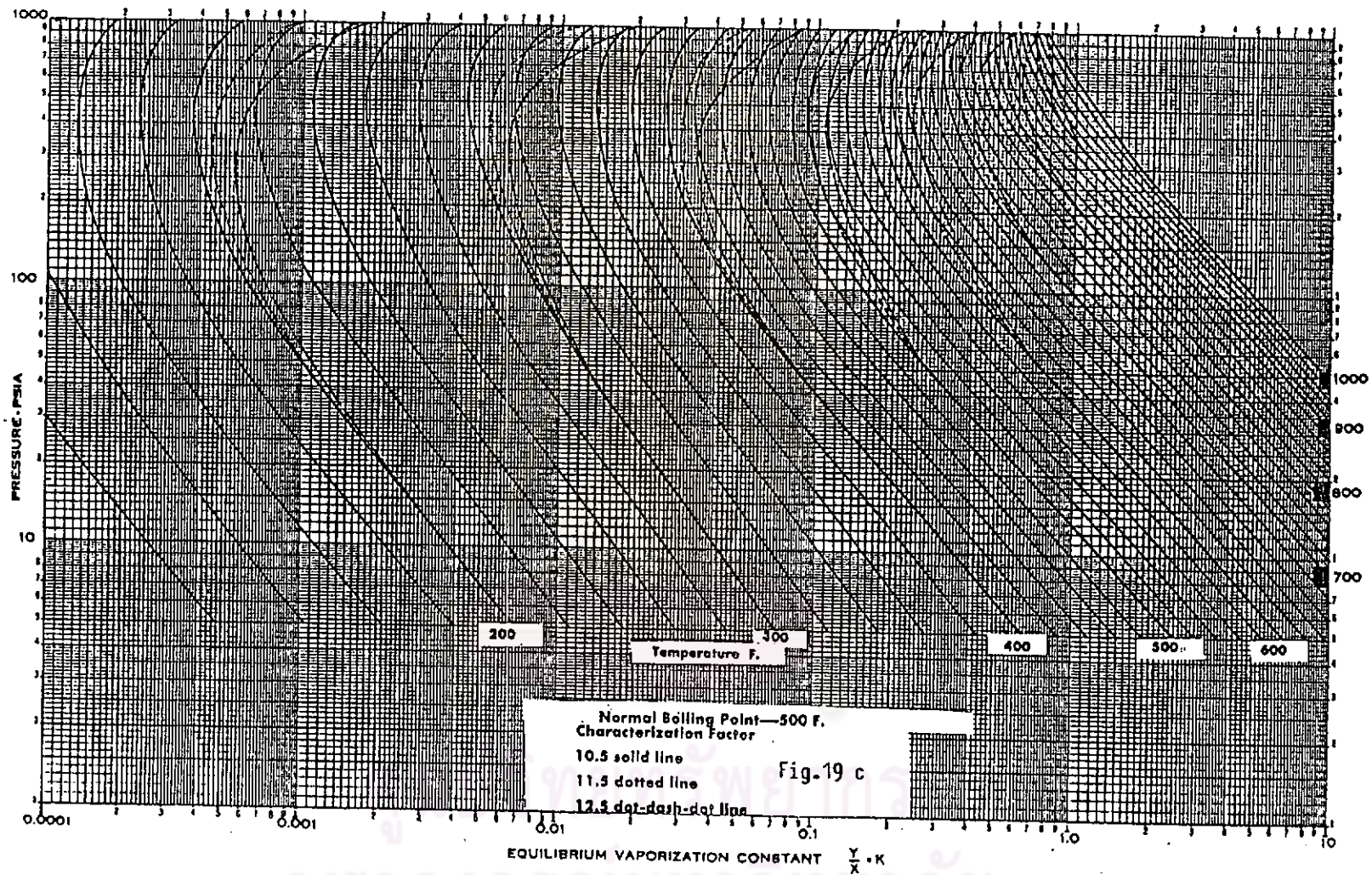
Only one source of experimental data has been found: White and Brown (59), covering naphtha and furnace oil fractions at 200 to 600 psig and 580°F to 800°F. The Hadden and Grayson (60) petroleum fraction K- correlations as shown in Fig.20, were made to fit these data.

None of these correlations could be used without wide extrapolation for crude oils, many of whose TBP curves extend to 1,500°F or higher. The only way to estimate the vaporization characteristics of high-boiling petroleum fractions was through the use of a vapor pressure chart, for which Maxwell and Bonnell Chart



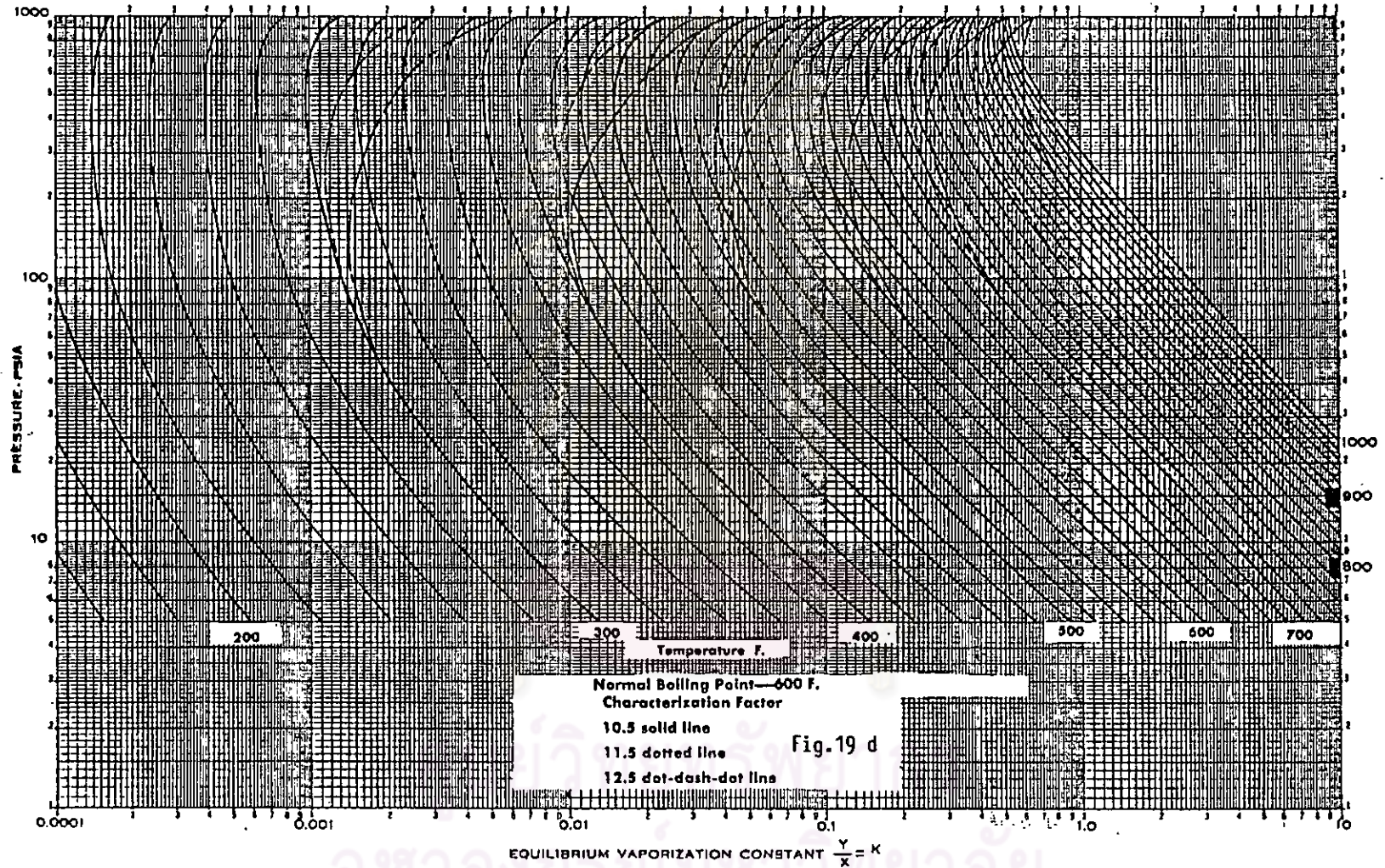


จุฬาลงกรณ์มหาวิทยาลัย

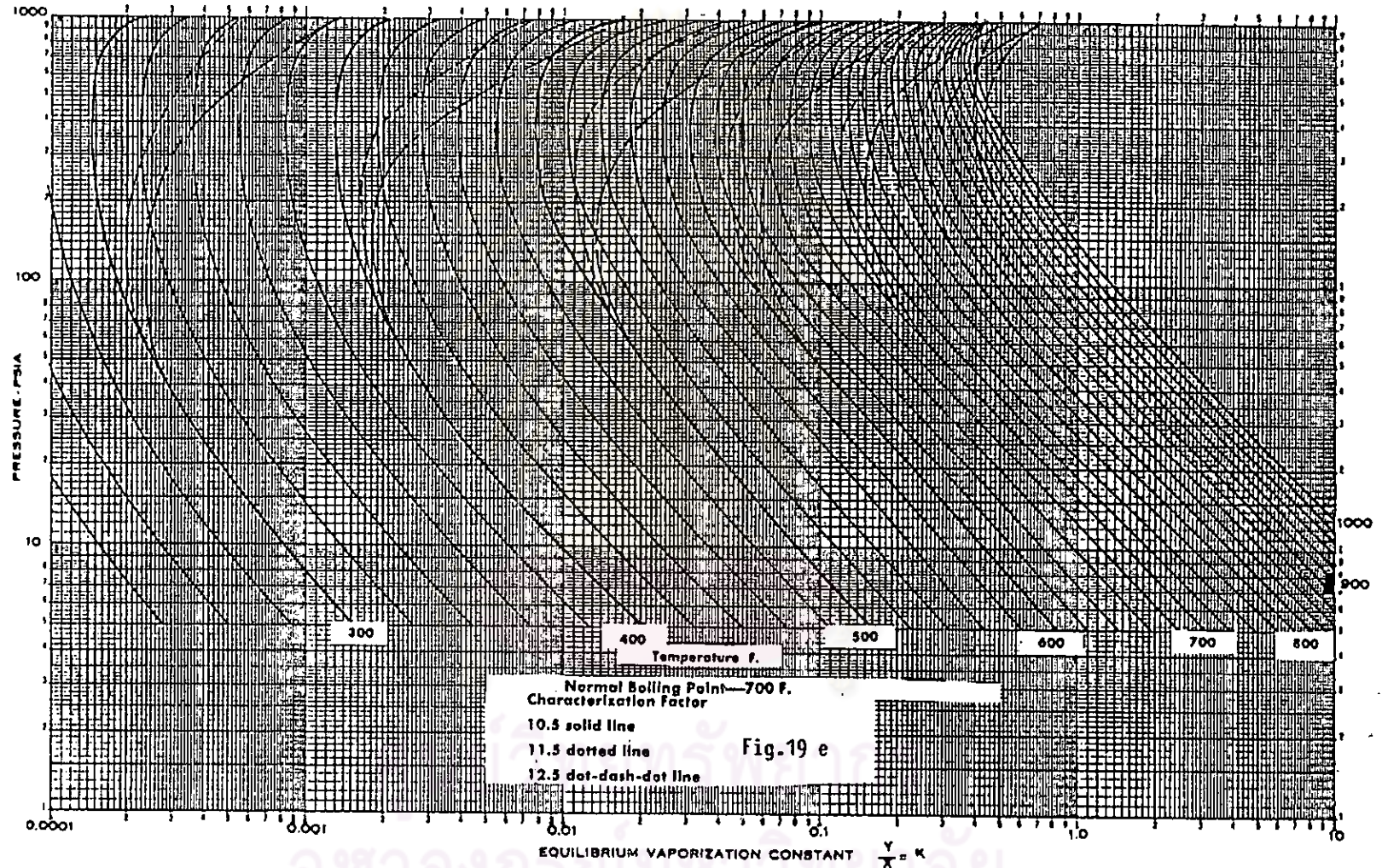


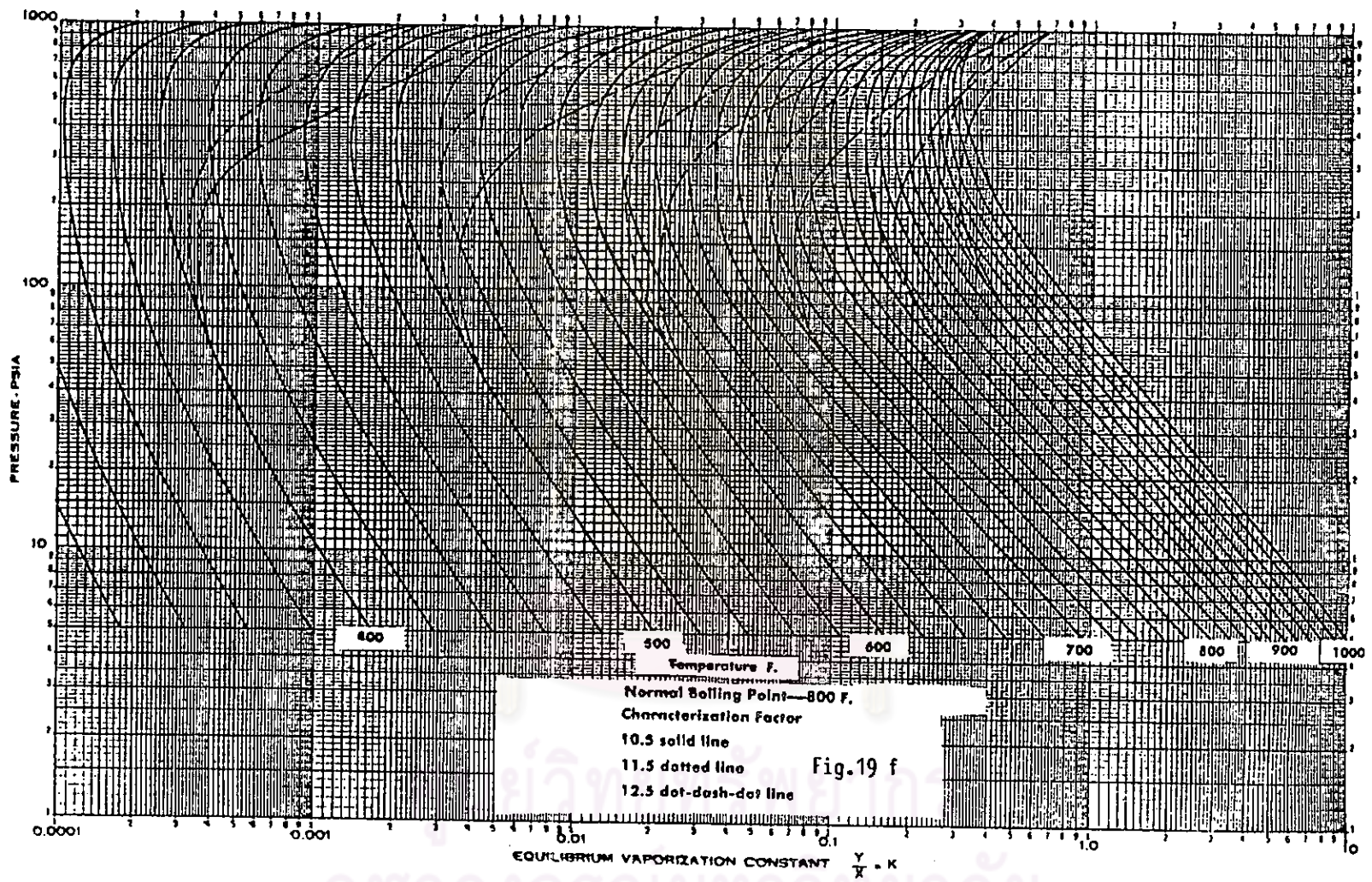
จุฬาลงกรณ์มหาวิทยาลัย



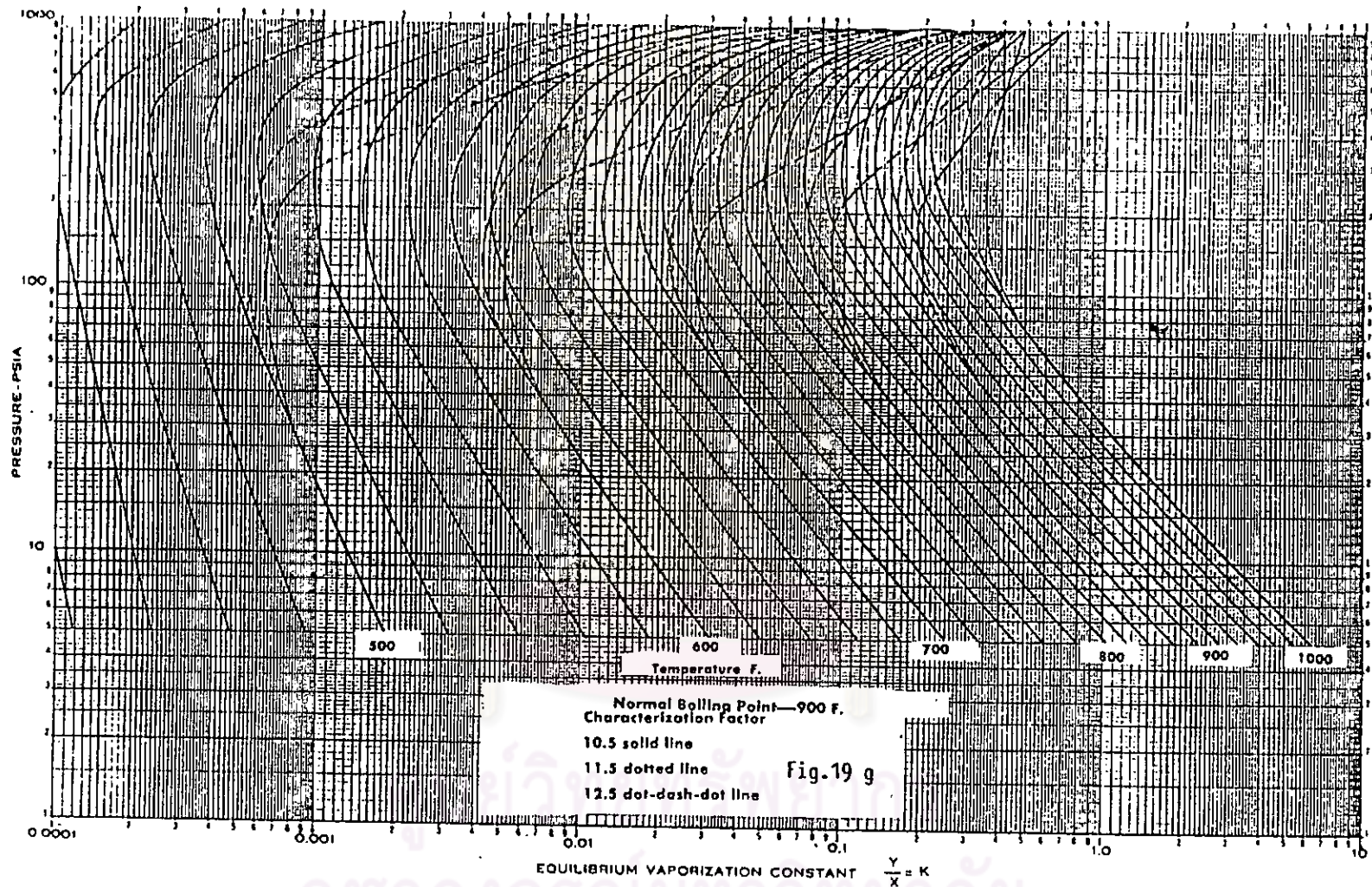


จุฬาลงกรณ์มหาวิทยาลัย

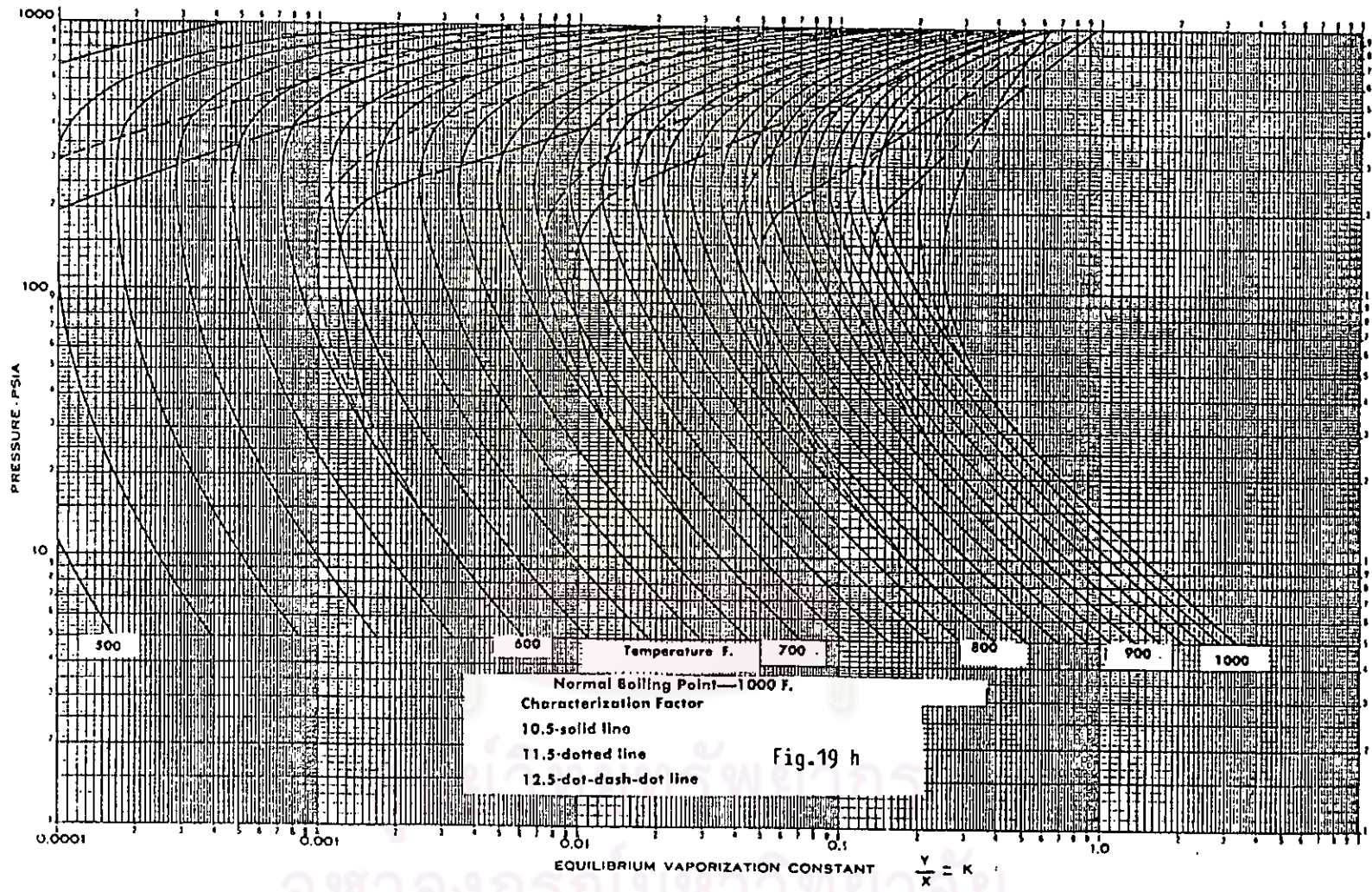




จุฬาลงกรณ์มหาวิทยาลัย



จุฬาลงกรณ์มหาวิทยาลัย



จุฬาลงกรณ์มหาวิทยาลัย

A COMPARISON OF ABOUT 900 EXPERIMENTAL POINTS WITH THE NOMOGRAM INDICATES THE FOLLOWING DEVIATIONS:
 STANDARD DEVIATION = 9.4%
 AVERAGE DEVIATION = 6.8%
 BIAS = +2.0%

$$\% \text{ DEVIATION} = \frac{K_{NOMO} - K_{EXP}}{K_{EXP}} \times 100$$

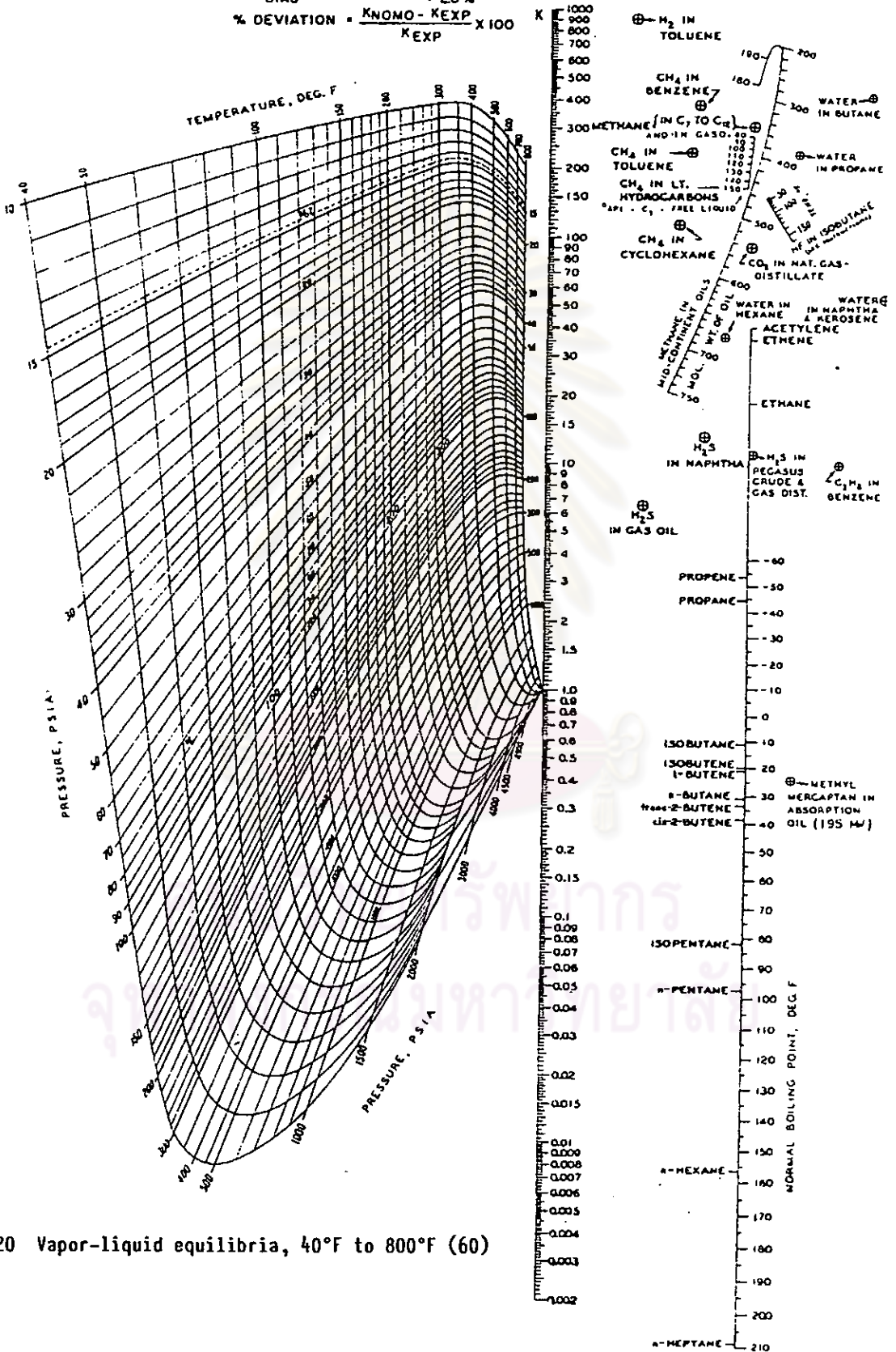


Fig.20 Vapor-liquid equilibria, 40°F to 800°F (60)

(42), also called the Esso 53-12 Chart (Fig.21) was recommended (38). The Raoult's Law K's ($K = \text{vapor pressure}/\text{total pressure}$) using the Esso 53-12 Chart gave the best results in a comparison test (38) at atmospheric pressure and under vacuum against the Raoult's Law K's corrected for vapor and liquid fugacity by the method in Edmister(43) and against the Hadden-Grayson K's up to 800°F boiling point, extrapolated up to higher boiling points by the fugacity K's.

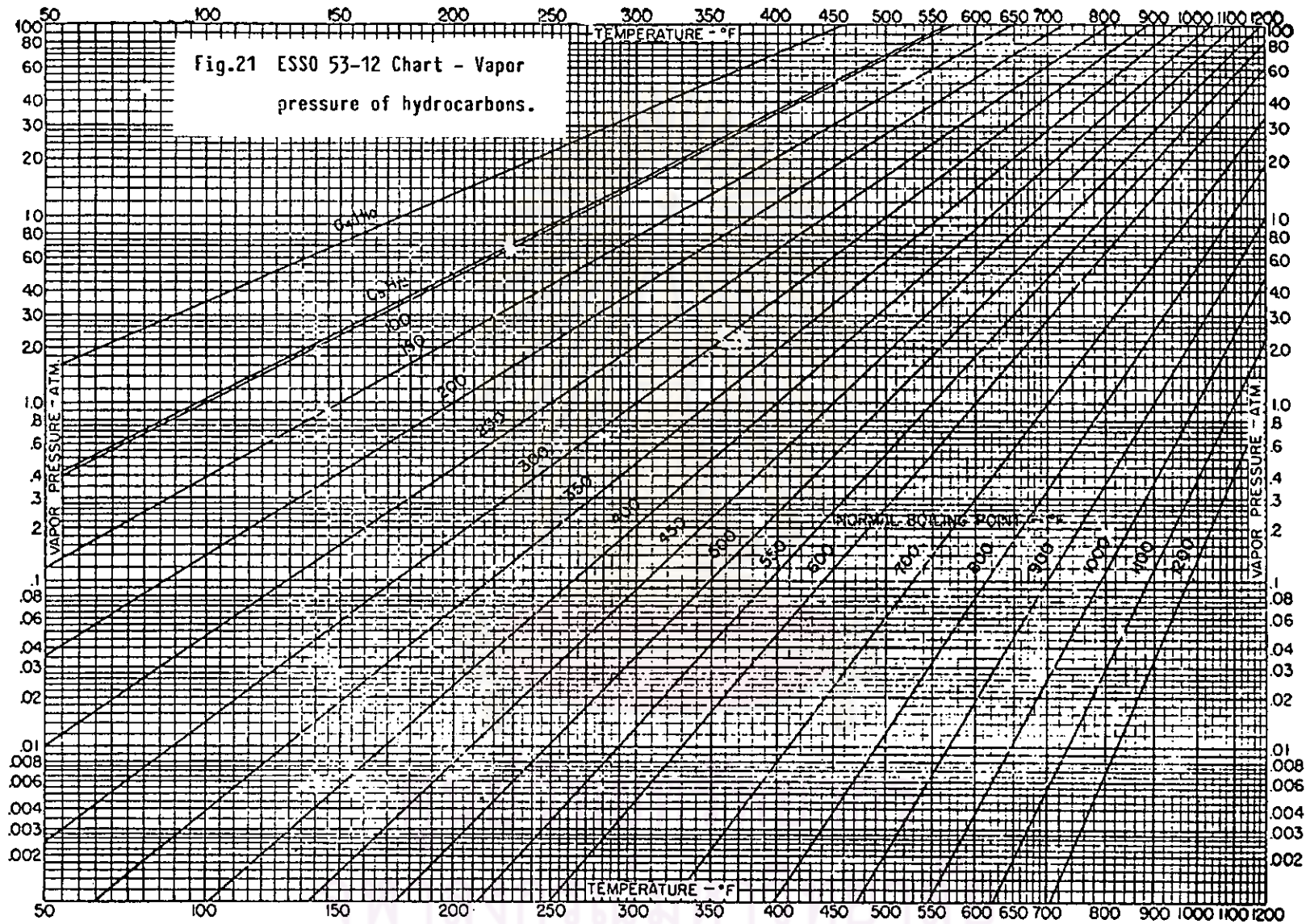
An equation has already been developed that fits the Esso 53-12 Chart over the entire range. It is

$$\log_{10}P = \sum_{i=0}^6 C_i \left(\frac{T'_B/T - 0.0002867T'_B}{748.1 - 0.2145T'_B} \right)^i \quad (14)$$

where P = Vapor pressure, mm.Hg
 T'_B = Normal boiling point corrected to UOP-K of 12.0, °R
 T = System temperature, °R
 C_0 = +6.769296
 C_1 = -3.567042×10^3
 C_2 = $+1.054060 \times 10^6$
 C_3 = -4.538994×10^8
 C_4 = -1.583831×10^{10}
 C_5 = $+3.861961 \times 10^{13}$
 C_6 = -5.487237×10^{15}

The term in the brackets was given in Maxwell and Bonnell's paper(42). The curve fit between $\log_{10}P$ and this term was developed by Hariu and Sage (38).

A correction is made to the vapor pressure for UOP-K,





according to Maxwell and Bonnell, by

$$T'_B = T_B - 2.5(UOP-K - 12.0)\log_{10}(P/760) \quad (15)$$

The calculation is iterated by finding a P from T_B via Eq.(14), adjusting T_B via Eq.(15) and repeating until the fractional change in P is less than a specified value. Then the K -value is calculated by dividing P by total pressure.

4.1.5 Vapor and Liquid Enthalpies

Various charts and graphs have been developed to provide basic enthalpy-temperature correlations for petroleum fractions; such parameters as average boiling point, or density in degrees API are commonly used. Additionally, graphs have been published for pressure correlations to the basic enthalpy data. Thus historically, the procedure for obtaining enthalpy data has been one of numerous steps usually involving the selection of an appropriate chart, and the making of one or more corrections to the basic data.

The enthalpy chart published by Bauer and Middleton (61) correlates the enthalpy of vapor and liquid petroleum fractions as a function of temperature and density in degrees API. Separate graphs for characterization factor and pressure corrections are provided on the same chart. Although these corrections provides reliable enthalpy data for most applications, the authors indicated that the reliability decreased markedly in the critical region. The critical region, however, is not indicated on their chart.

The critical region is, however, defined clearly in

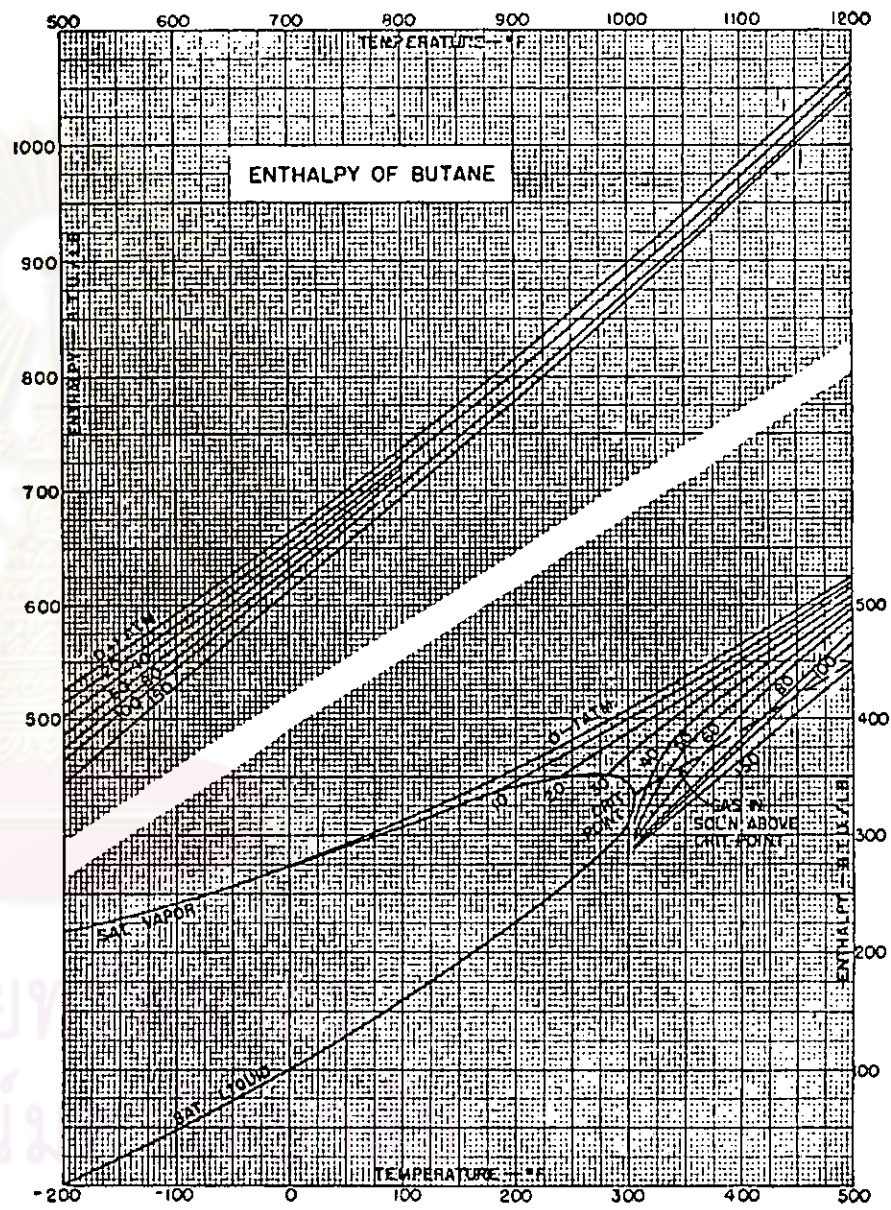
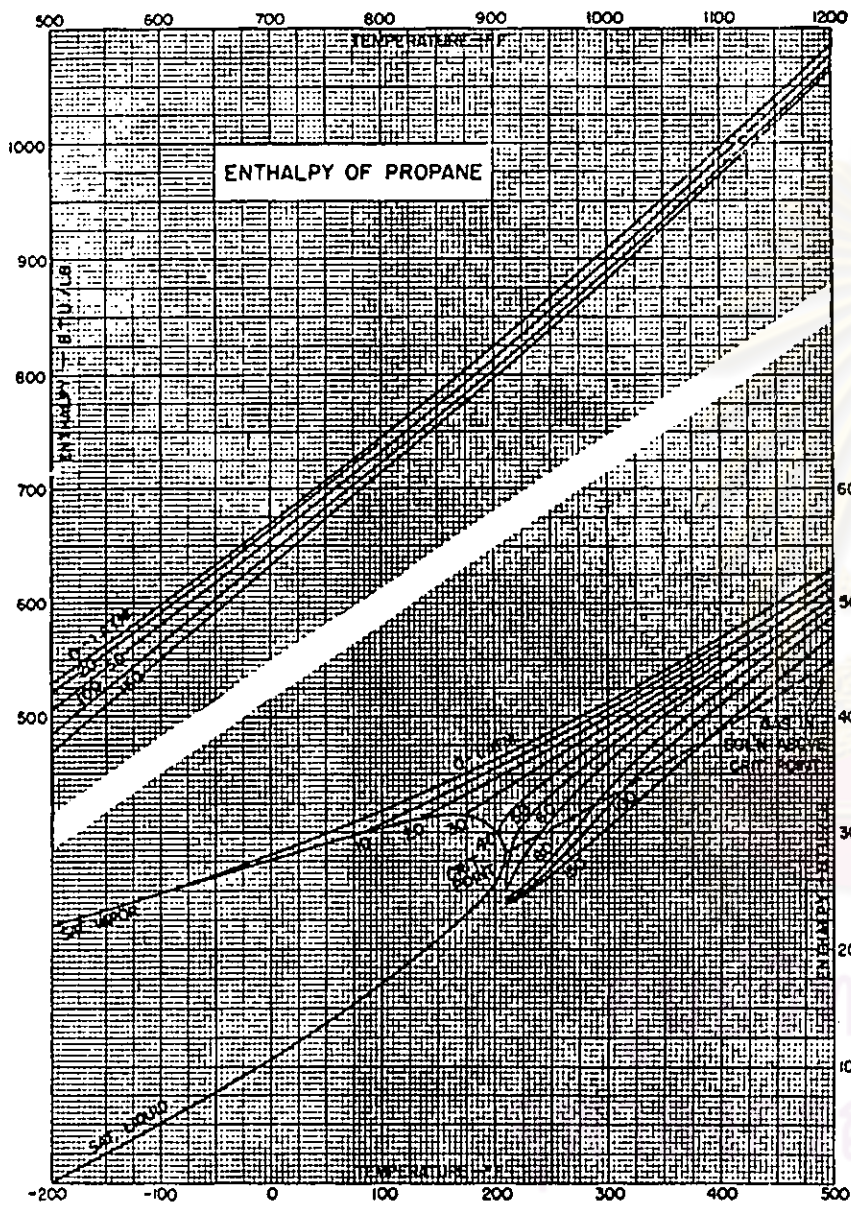


Fig.22b

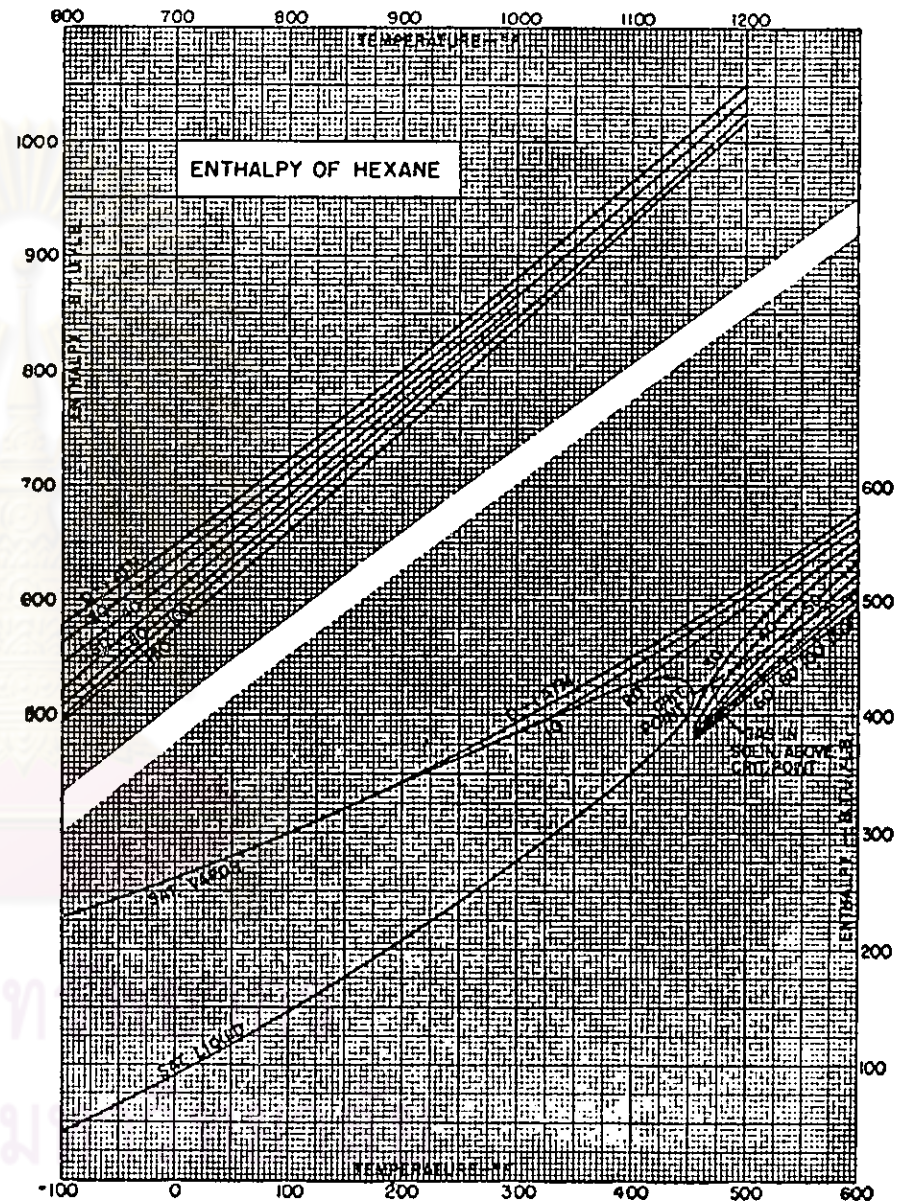
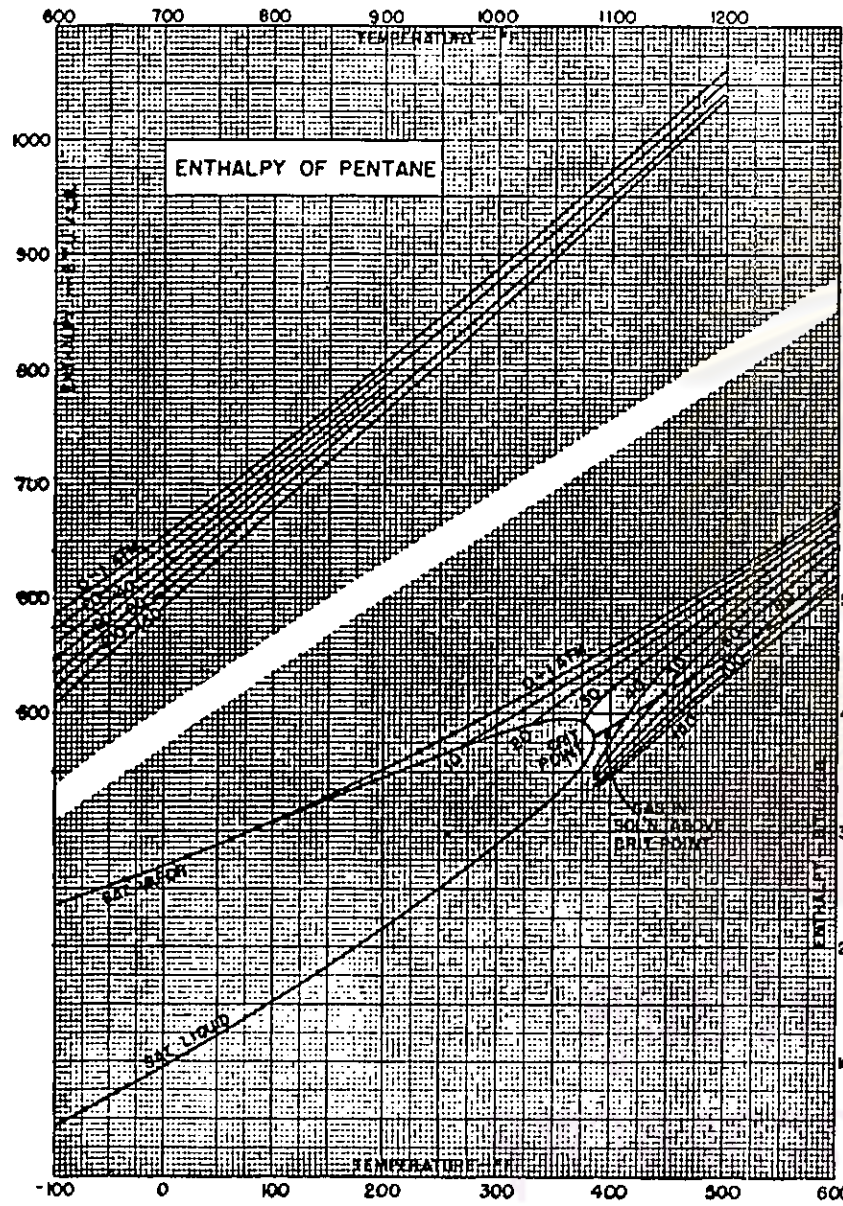


Fig.22c.

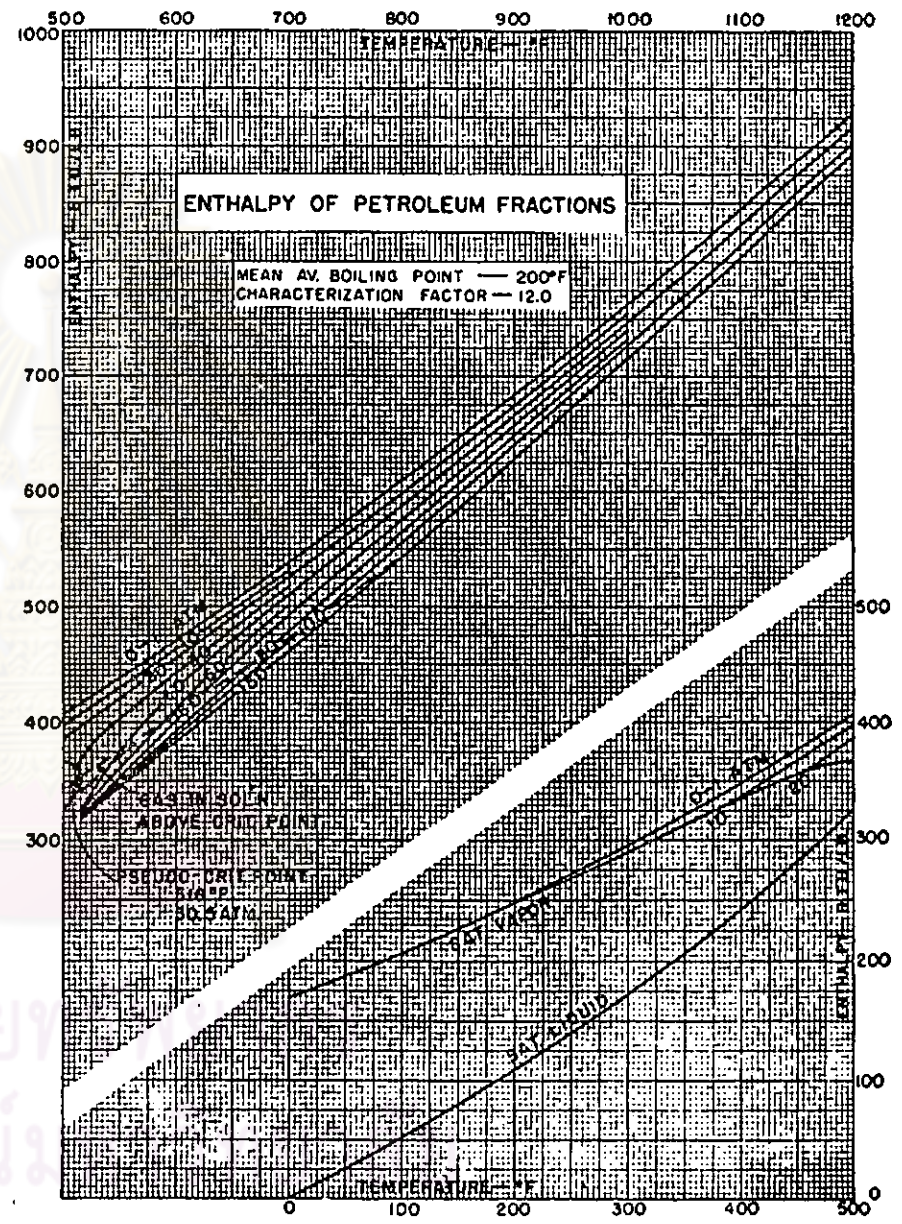
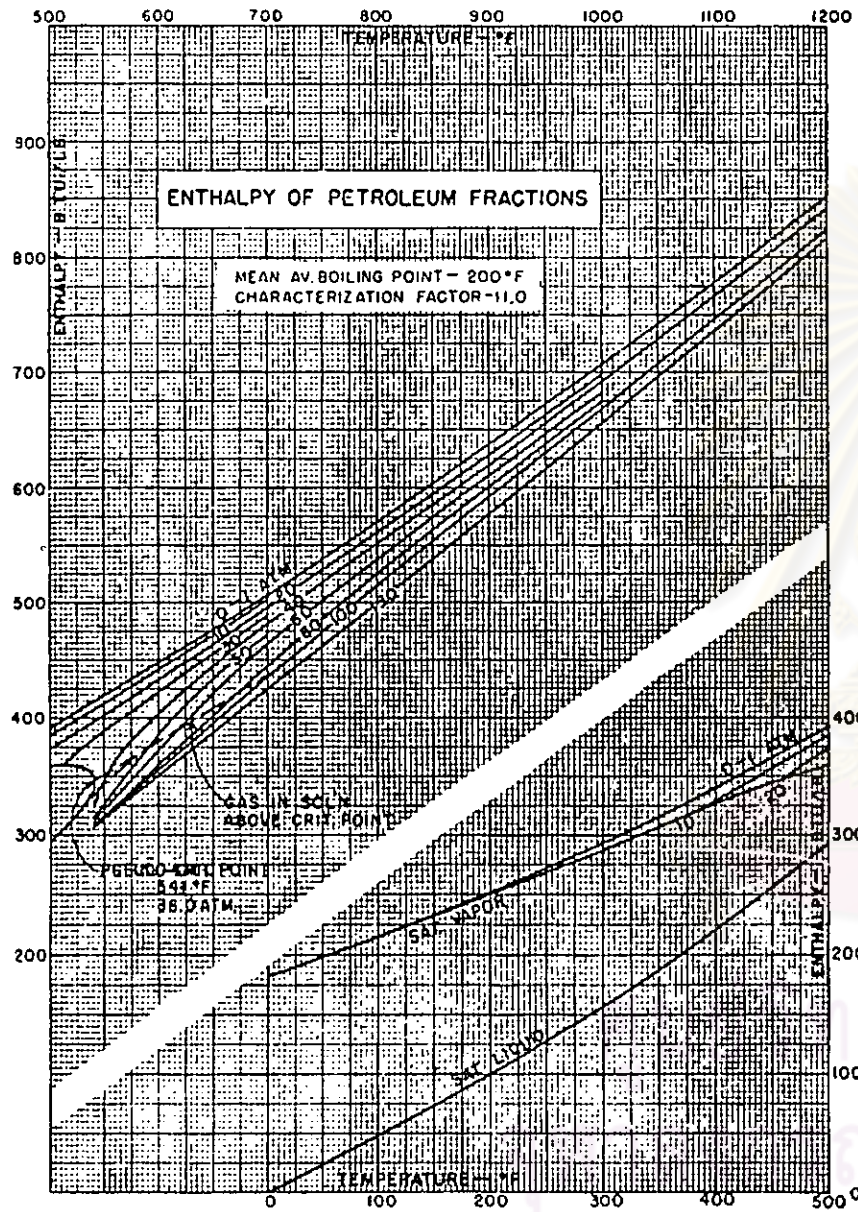


Fig.22e

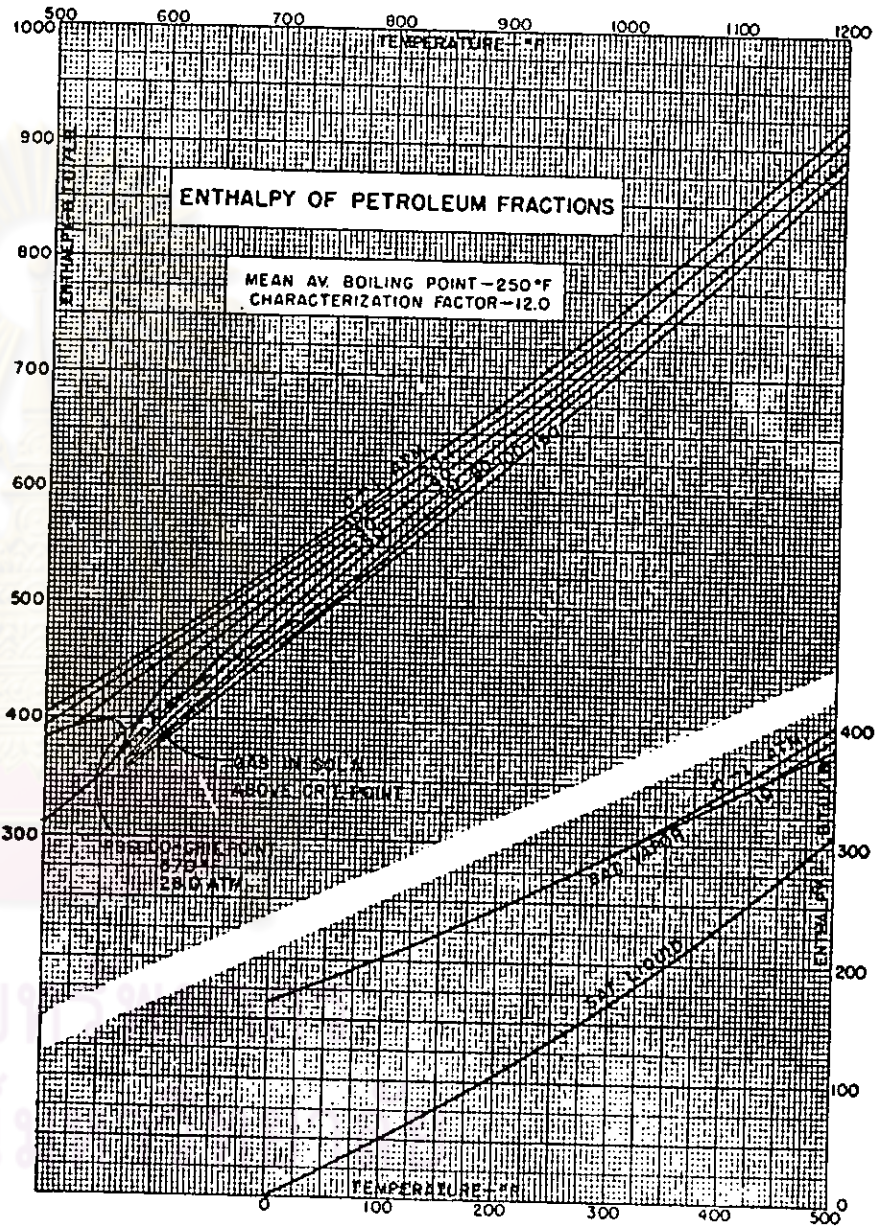
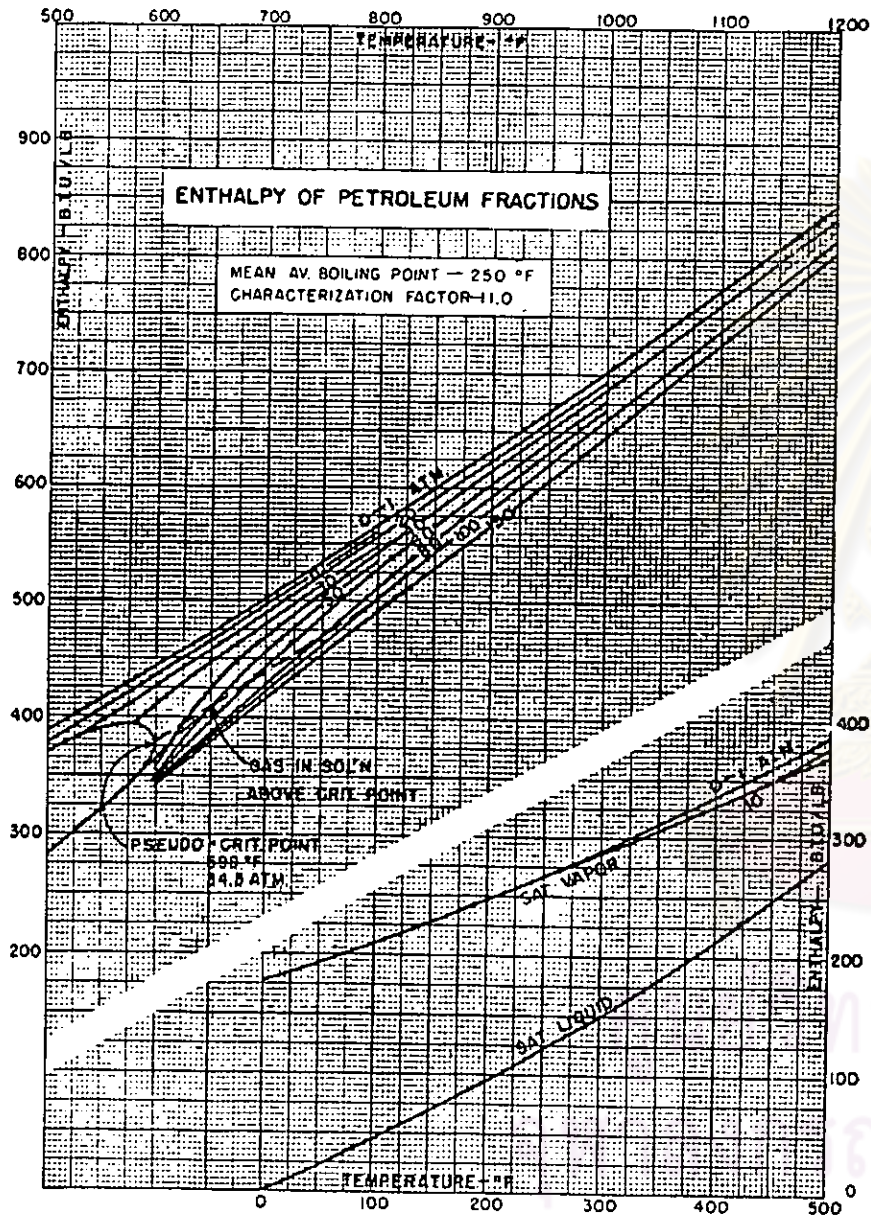


Fig.22f

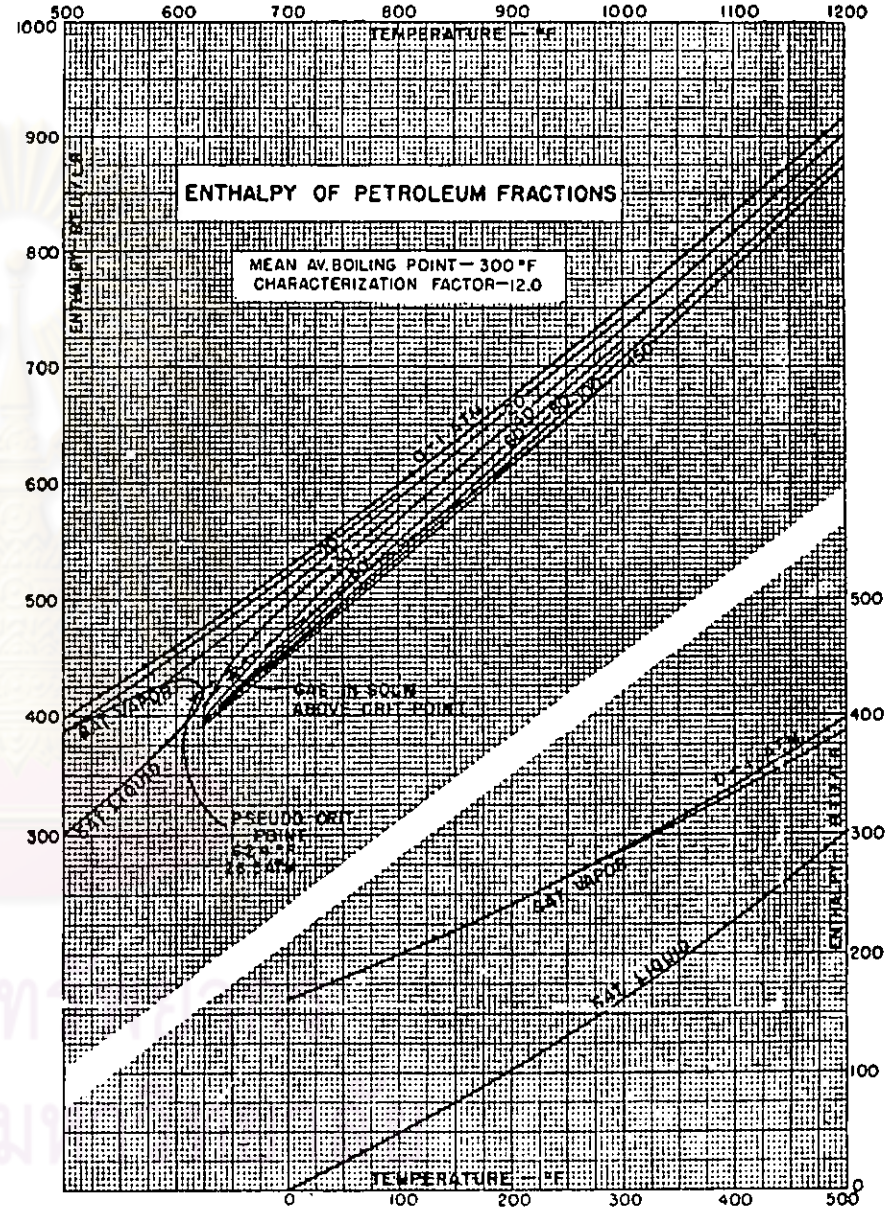
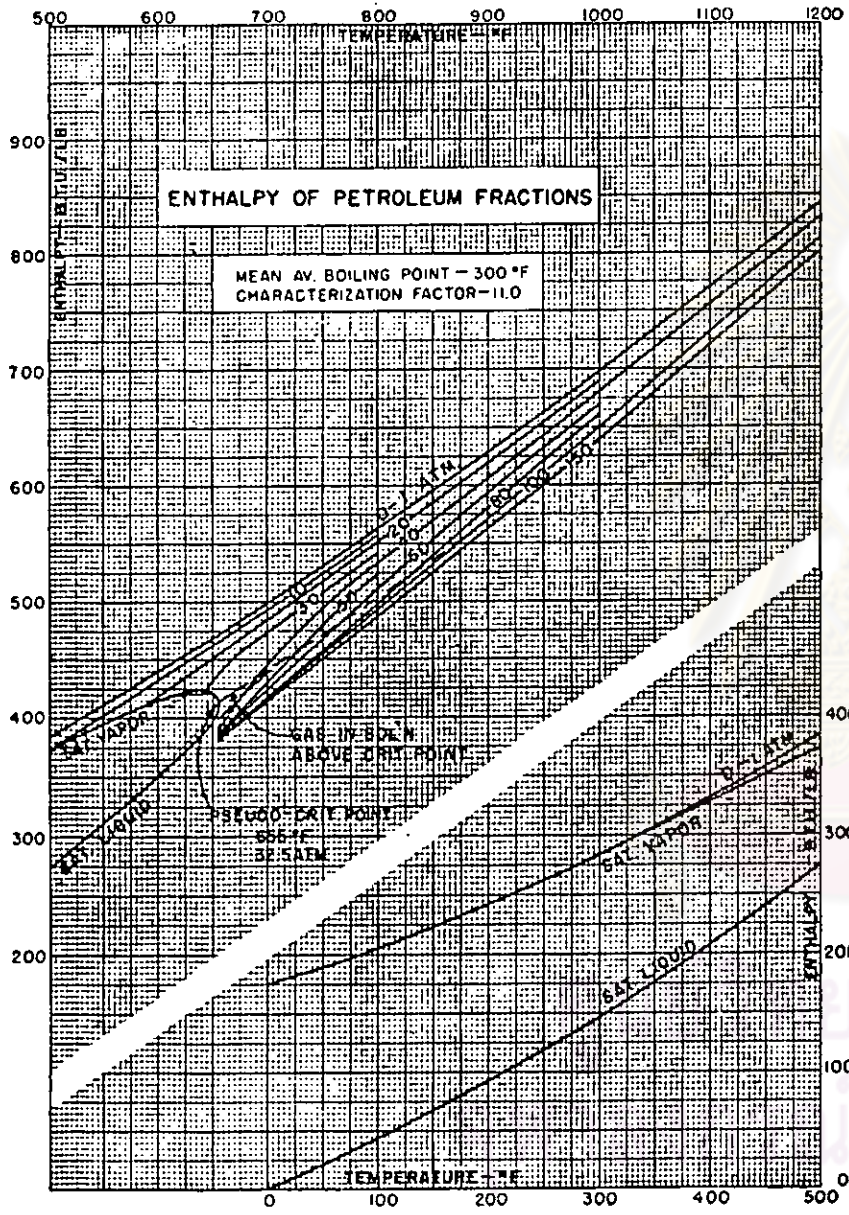


Fig.22g

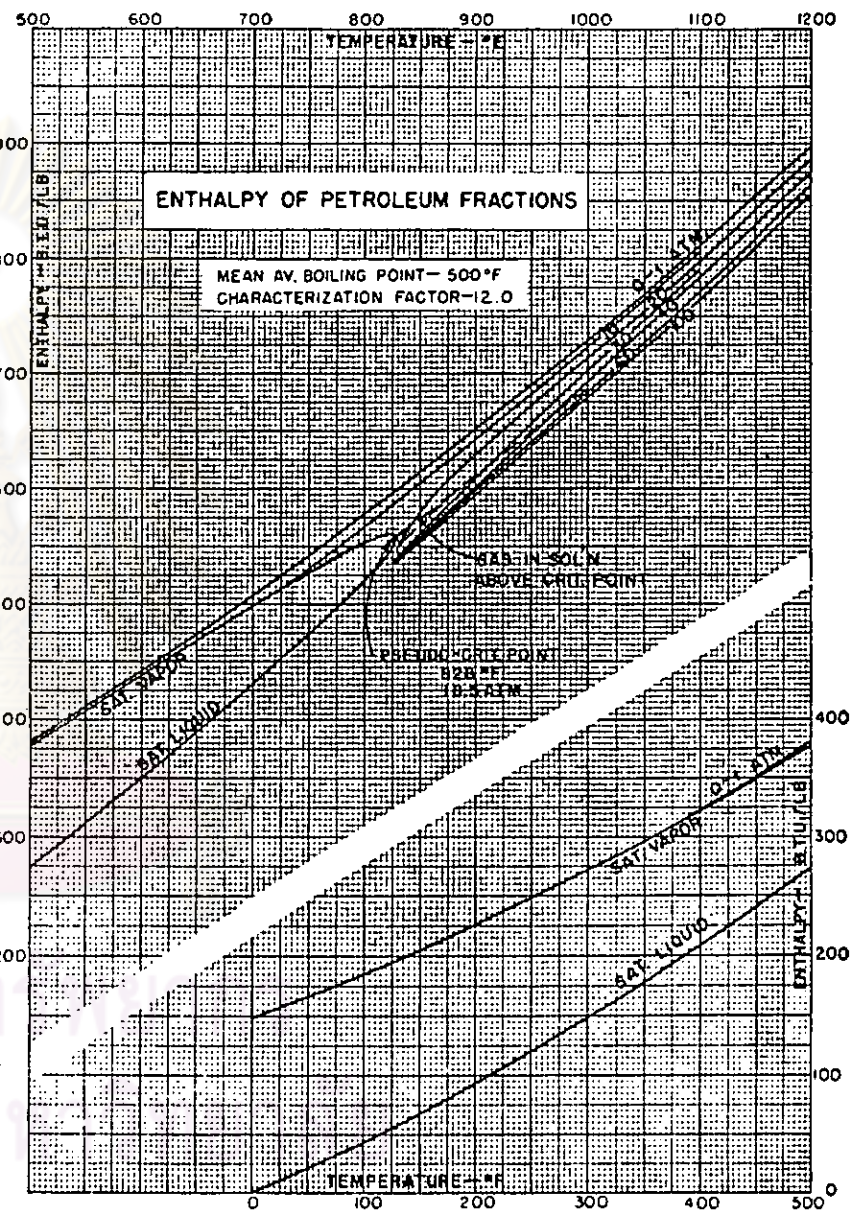
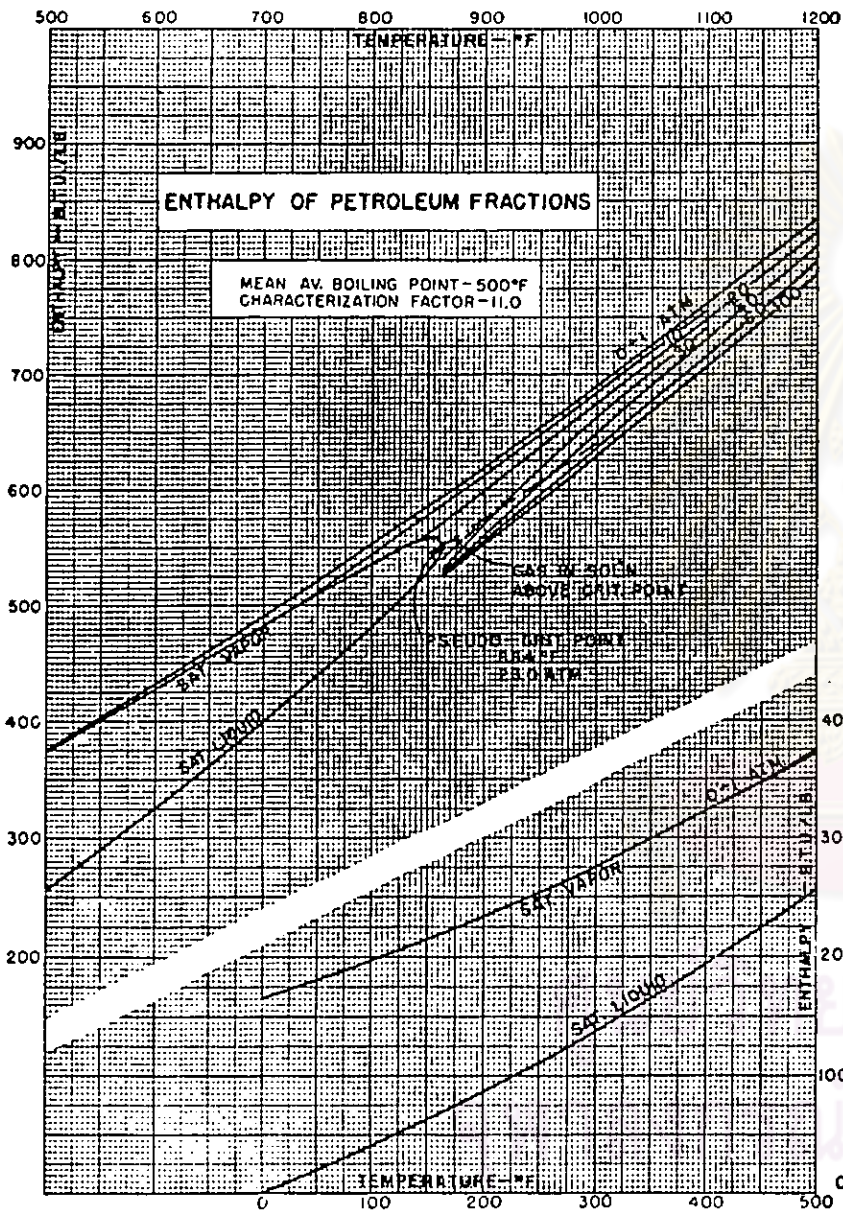


Fig.22i

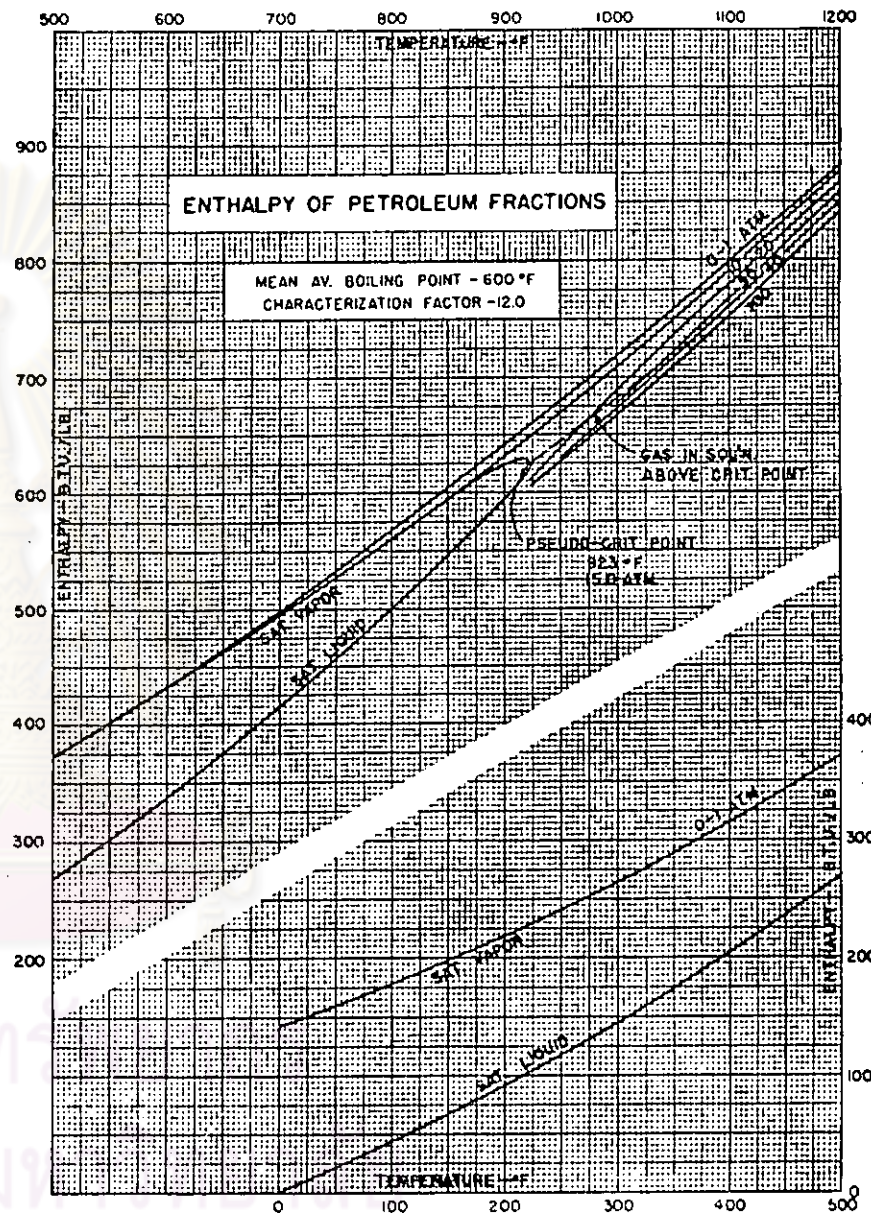
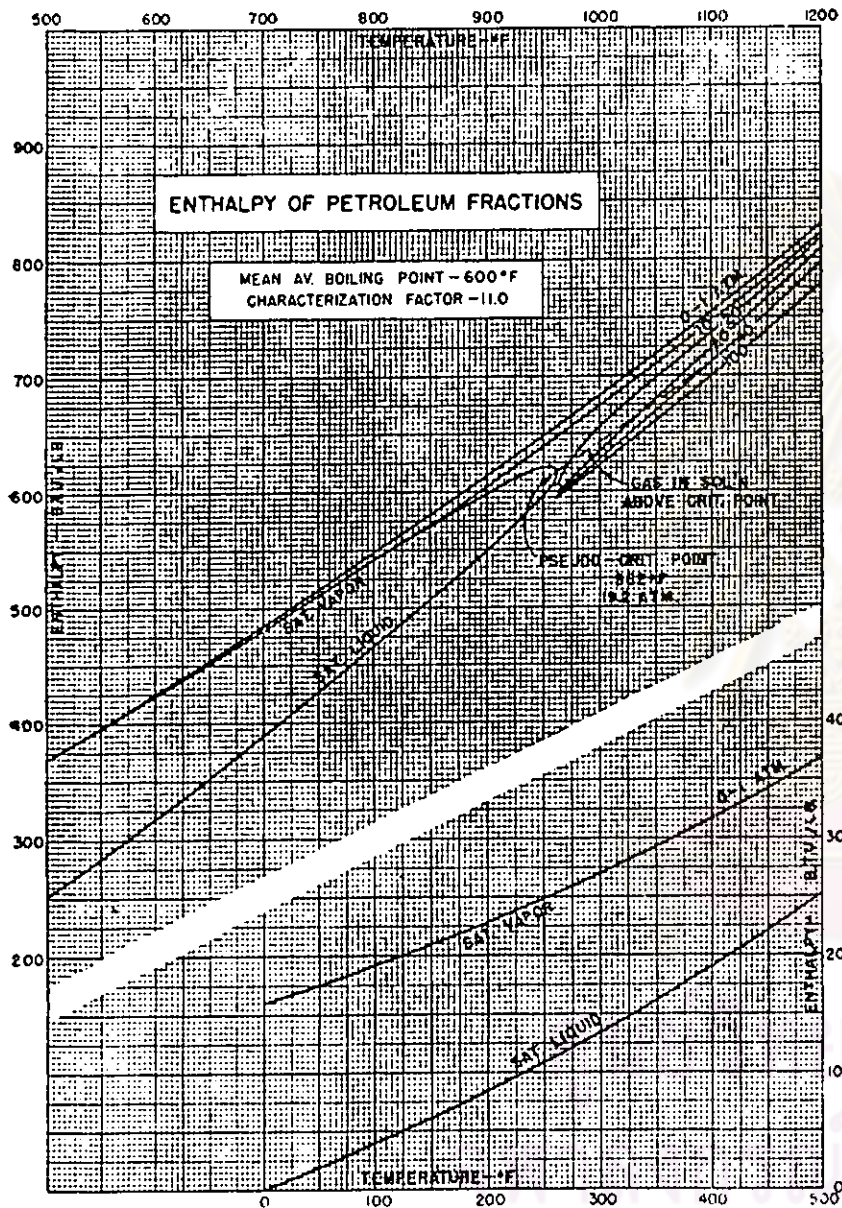


Fig. 22j

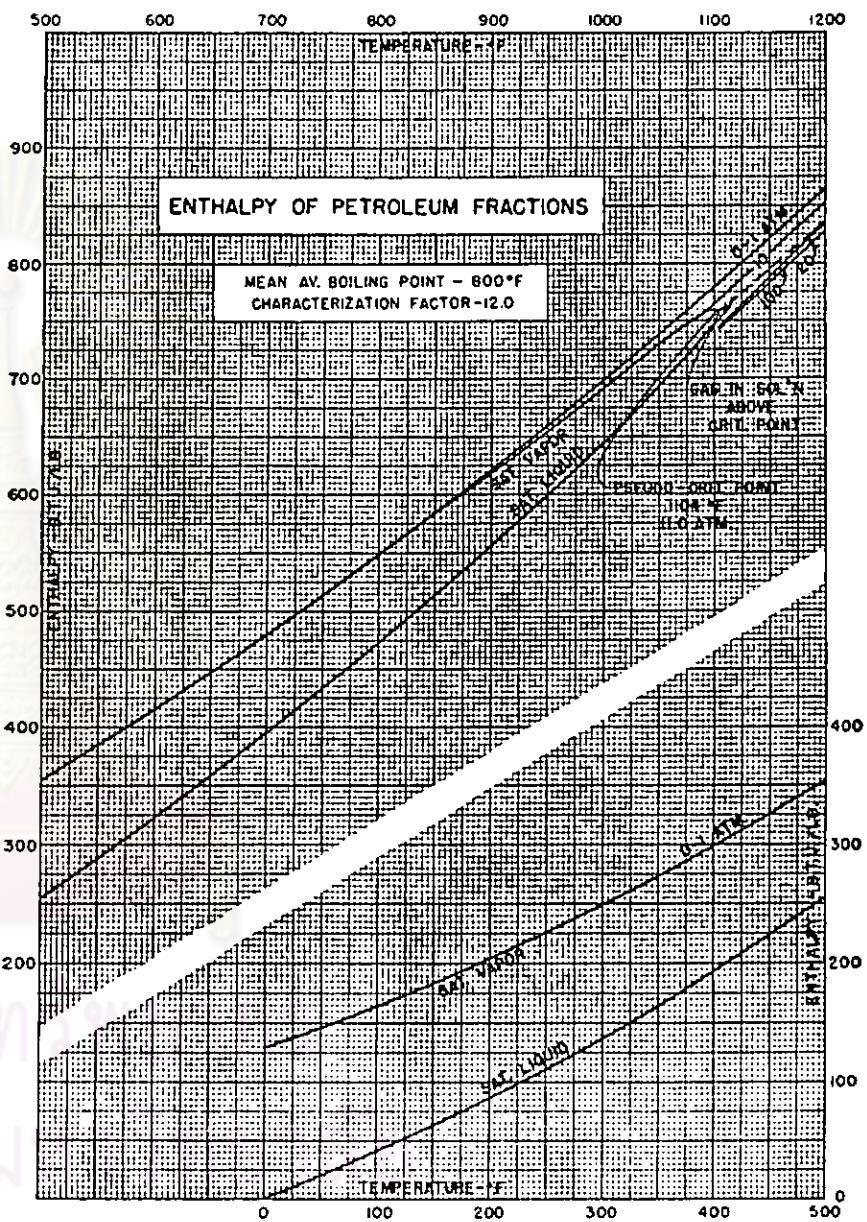
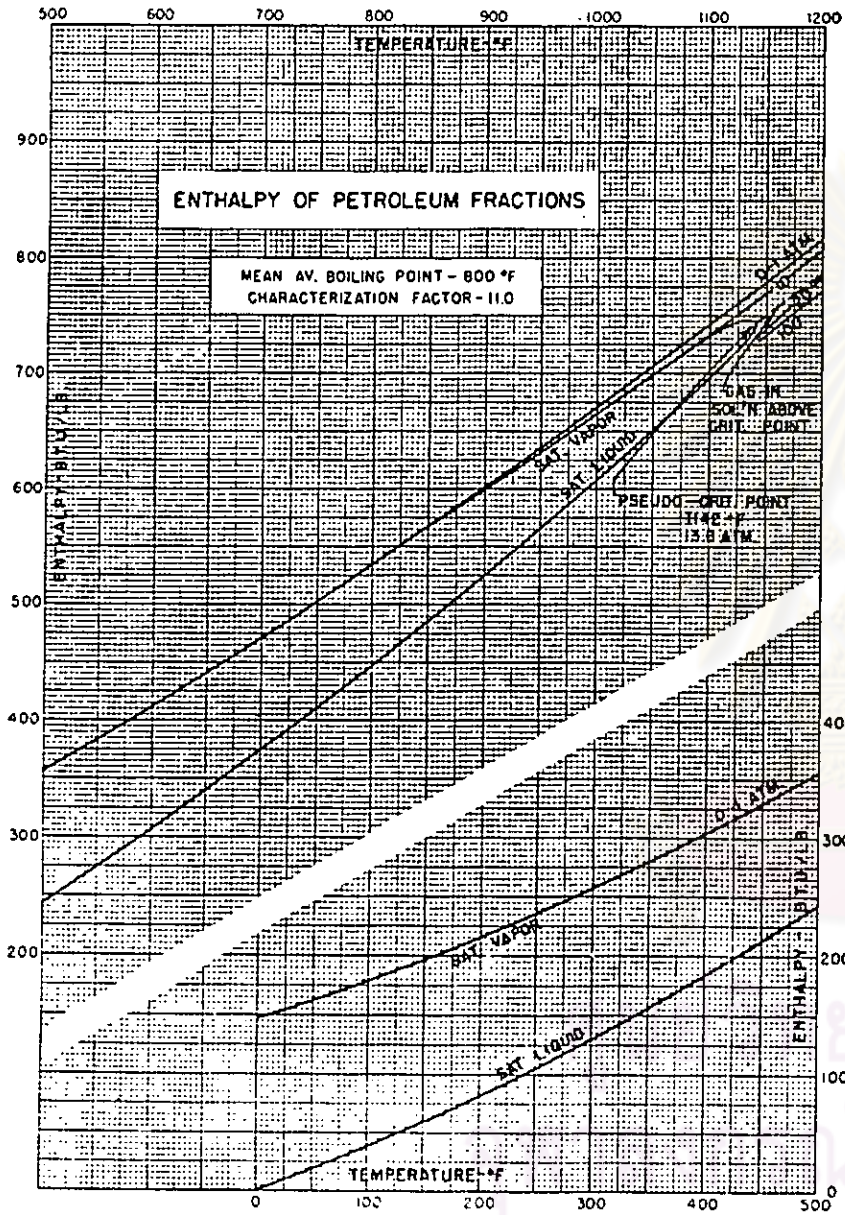
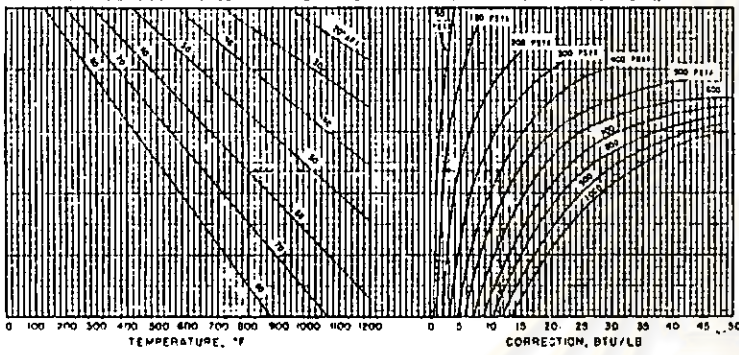


Fig.22k

700 800 900 1000 1100 1200

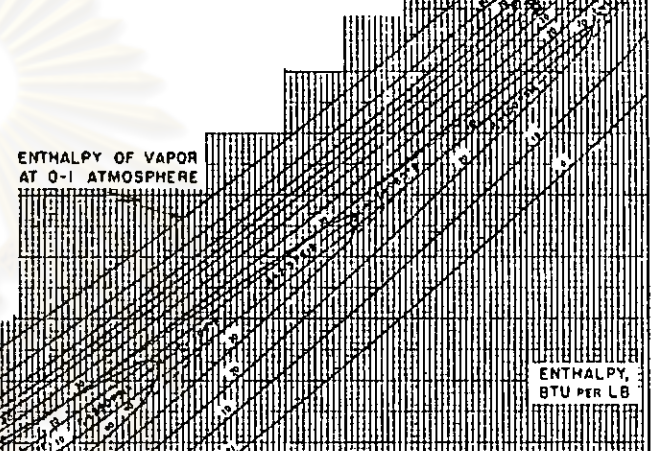
**PRESSURE CORRECTION FOR ENTHALPY OF VAPOR: UOP "K" - 11.8
(TO BE SUBTRACTED FROM ENTHALPY OF VAPOR AT 0-1 ATMOSPHERE)**



NOTE: THIS PRESSURE CORRECTION CHART IS CONVENIENT AND FAIRLY ACCURATE. ABOVE AND BELOW THE CRITICAL REGION, THE DEVIATION FROM CALCULATED CORRECTIONS (SOURCE 2) IS GENERALLY LESS THAN 2.0 BTU'S PER POUND. IN THE CRITICAL REGION HOWEVER (A BETWEEN 0.8 AND 1.2), THE DEVIATION MAY BE AS HIGH AS 15 BTU'S PER POUND. FOR MORE ACCURATE CORRECTIONS AND CORRECTIONS BEYOND THE RANGE OF THIS CHART, SEE THE REDUCED PROPERTY SERIES FIGURES 6 & 7

**Fig.23
ENTHALPY OF
PETROLEUM FRACTIONS (62)**

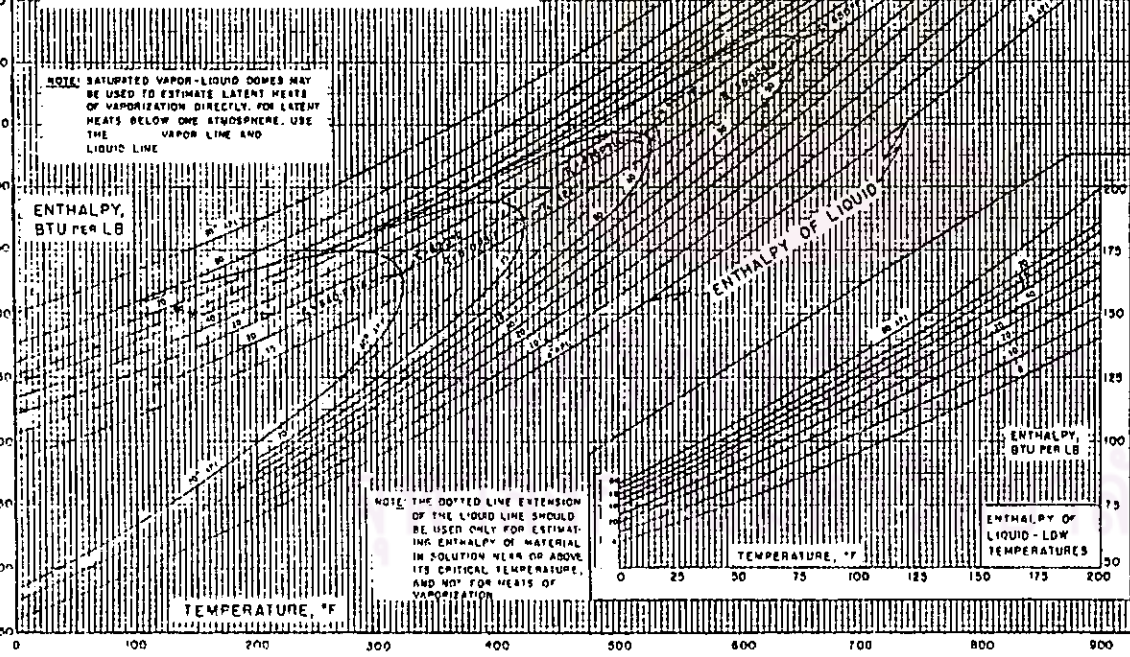
ENTHALPY OF VAPOR AT 0-1 ATMOSPHERE



ENTHALPY, BTU PER LB

NOTE: SATURATED VAPOR-LIQUID DOWNS MAY BE USED TO ESTIMATE LATENT HEATS OF VAPORIZATION DIRECTLY. FOR LATENT HEATS BELOW ONE ATMOSPHERE, USE THE VAPOR LINE AND LIQUID LINE

ENTHALPY, BTU PER LB



NOTE: THE DOTTED LINE EXTENSION OF THE LIQUID LINE SHOULD BE USED ONLY FOR ESTIMATING ENTHALPY OF MATERIAL IN SOLUTION NEAR OR ABOVE ITS CRITICAL TEMPERATURE, AND NOT FOR HEATS OF VAPORIZATION

TEMPERATURE, °F

ENTHALPY OF LIQUID - LOW TEMPERATURES

NOTE: THIS CHART IS APPLICABLE FOR A.S.F.M. SLOPES < 2.0

EXAMPLES:

1. FIND THE LATENT HEAT OF VAPORIZATION OF A 60° API OIL AT 800°F AND 400 PSIA
SOLUTION: USING THE ABOVE FOR 60° API STOCK, READ ENTHALPIES OF SATURATED VAPOR AND LIQUID DIRECTLY. NO PRESSURE CORRECTION IS NECESSARY.
 $H_v = 448 \text{ BTU/LB}$
 $H_l = 385$
 $\Delta H = 67 \text{ BTU/LB}$

2. FIND THE ENTHALPY OF A VAPOR GIVEN THE CONDITIONS:
 $T = 60^\circ \text{ A.P.I.}$ $T = 800^\circ \text{ F}$
 $K = 11.8$ $P = 400 \text{ PSIA}$

SOLUTION
 ENTHALPY OF VAPOR AT 0-1 ATMOSPHERE 378 BTU/LB
 PRESSURE CORRECTION -11
 ENTHALPY OF VAPOR AT 800°F AND 400 PSIA 367 BTU/LB

**ENTHALPY OF PETROLEUM FRACTIONS
UOP "K" - 11.8
BASIS: LIQUID AT 200°F**

SOURCE: DEVELOPED FROM THE SOURCE: MIDDLETON, M.E. 1958
 REF. JAN. 1953
 (21) LINDSEY ET AL. UNIV. OF WISCONSIN, REP. NO. 4, OCT. 1953

Maxwell's (44) series of dome charts for the enthalpy of petroleum fractions (Fig.22a-k). Separate charts are shown for petroleum fractions of various average boiling points, generally in 100 degree increments, and each of these is represented at characterization factors of 11.0 and 12.0.

The enthalpy chart published by Johnson and Grayson (62) incorporates the advantages of both the aforementioned publications and eliminates most of the disadvantages. The enthalpy chart presented in Fig.22 was adapted and developed primarily from data presented by Bauer and Middleton (61) and Lyderson et al.(63). The enthalpy of vapor is presented at zero absolute pressure. For most conditions, the zero-pressure data can be used for pressures up to about 50 psia before corrections become significant. The enthalpy of vapor at zero absolute pressure and liquid at one atmosphere is taken directly from the Bauer-Middleton data except that the basis is changed from liquid at 0°F to liquid at -200°F. The zero-pressure vapor enthalpies reproduce the experimental data within about +5 Btu/lb.

4.2 Topping Column Models

In order to simulate a topping column, the "theoretical analogue" of an actual column is first determined. The "theoretical analogue column" is defined as one which has the required number of theoretical (or perfect) plates between consecutive product withdrawal positions so as to obtain product streams that possess the same characteristics as those withdrawn from the actual column. In general, the theoretical analogue column is determined by reducing

the original number of plates between the product withdrawal positions, as possessed by the actual column, until the conditions of the above definition are satisfied. Once an analogue has been determined and confirmed with observed results, it can next be used to simulate other conditions for the given unit.

The mathematical model for the topping column in this work is an extension of the 2N-Newton-Raphson for absorbers as presented by Holland (2). As an illustration of the mathematical model, a theoretical analogue system as shown in Fig.24 is selected to describe and test the computer program. The distillation system has four sidestrippers connected to the main. The plates are numbered sequentially starting from the condenser-accumulator drum down to the last plate of the lowest stripper. The plate description is as follow:

Plate no. 1	condenser-accumulator
2	top plate of main column
NW(i)	sidestream withdrawal plate
NV(i)	plate below which vapor stream from sidestripper is returned
NP(i)	pumparound withdrawal plate
NQ(i)	plate to which liquid-pumparound stream is returned
NF	feed plate
NT	bottom plate of main column
NTOP(i)	top plate of each sidestripper
NBOT(i)	bottom plate of each sidestripper

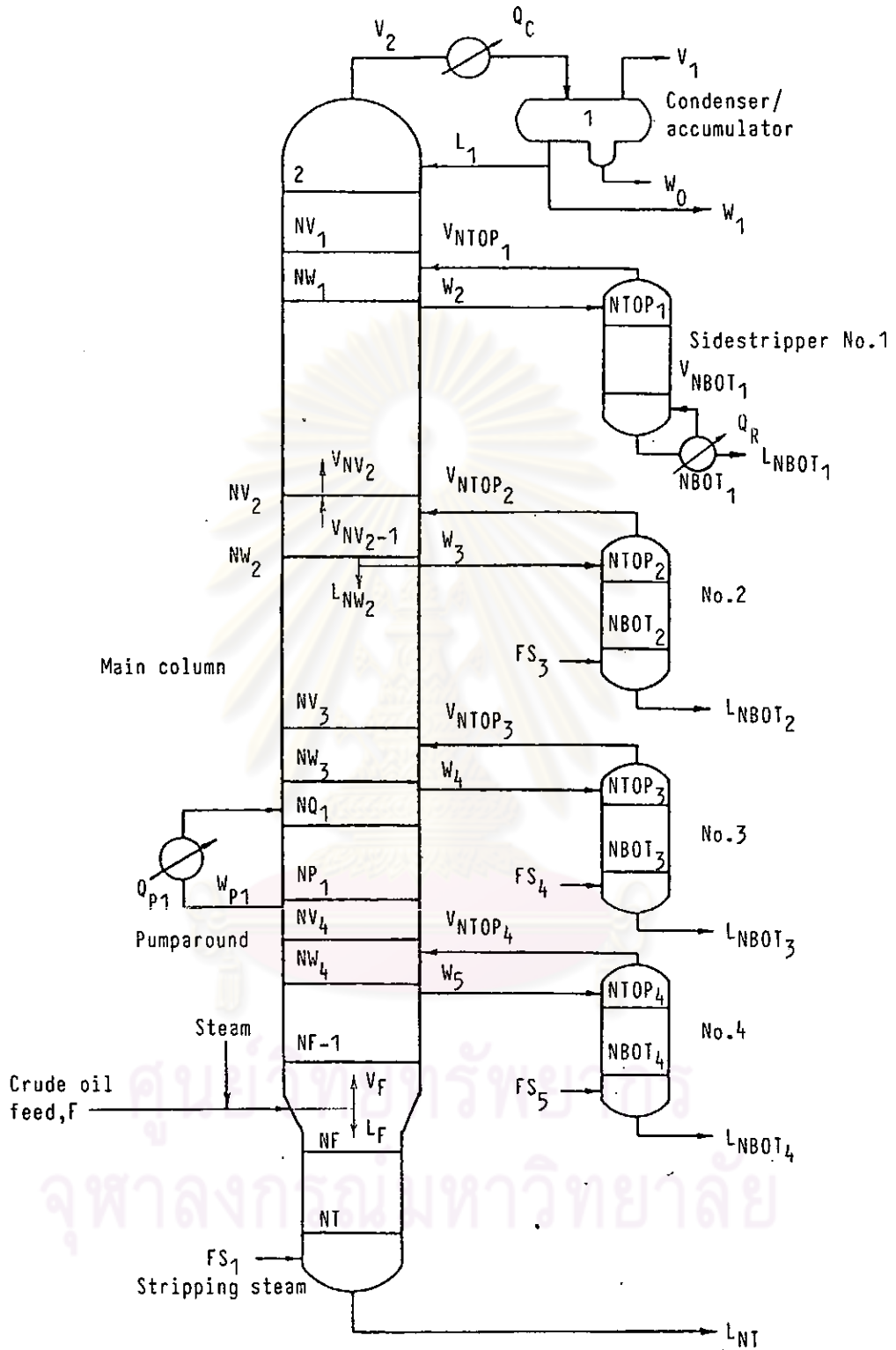


Fig.24 An illustrative theoretical analogue system for mathematical model presentation.

For this theoretical analogue column, the following variables are regarded as fixed:

a) The number of theoretical plates in the main column and sidestrippers as well as the locations of all stream withdrawals and return positions

b) Quantity, composition, and thermal conditions of all feeds

c) Column pressure and the pressure drop per stage

d) The overhead reflux ratio (or alternately, the condenser duty Q_C)

e) Distillate W_1 and sidestripper withdrawal rates L_{NBOT}

f) The boilup ratio for the reboiler-type side stripper (or alternately, the reboiler duty Q_R)

g) The intercooler duty Q_p for the pumparound stream W_p

h) The pumparound rate W_p and its withdrawal and return position

4.2.1 Choice of Independent Variables

The N -stage temperatures, T_j and the N -ratios of the total-flow rates, V_j/L_j , are selected as the independent variables in this formulation of the Newton-Raphson method. Alternatively, a heating or cooling duty may be selected instead as an independent variable, and the V/L for that stage specified. For example, by specifying of the reflux ratio V_1/L_1 , the condenser duty Q_C and the temperature T_1 become the independent variables for the first stage of the main column. The variable V_j/L_j is replaced by a new variable θ_j , which is defined as follows:

$$V_j/L_j = \theta_j (V_j/L_j)_a \quad (16)$$

where $(V_j/L_j)_a$ is any arbitrarily assumed value of V_j/L_j . Taking this assumed ratio to be the most recently found value of V_j/L_j in the iterative process serves to normalize the θ_j 's so that, at convergence, θ_j approaches unity for all j .

A new variable θ_0 is introduced to account for the two liquid phases in the accumulator. It is defined in a manner analogous to that for the remaining θ 's; namely,

$$W_0/V_1 = \theta_0 (W_0/V_1)_a \quad (17)$$

4.2.2 Total Material Balances

The total material balances may be stated in terms of the vapor flow rates V_j or the liquid flow rates L_j and the θ_j 's. In the statement of the total material balances, a multiplier R_j is introduced for the sake of simplicity. It is defined as follows:

$$V_j = R_j L_j \quad (18)$$

where $R_j = \theta_j (V_j/L_j)_a$, except for $j=0$ or plate where V/L is specified. For $j=0$, $R_0 = \theta_0 (W_0/V_1)_a$; and for any plate that V/L is specified, $R_j = V_j/L_j$.

It is simpler to formulate the total material balances in terms of L_j 's and the R_j 's (or θ_j 's) when the sidestripper withdrawal rates L_{NBOT} are known. The balances for plates 1, 3, NV, NW and NQ are made, and next the complete set of total material balances

are stated in matrix form.

a) Plate 1: The total material balance enclosing the condenser-accumulator section is given by

$$V_2 - V_1 - L_1 - W_0 - W_1 = 0 \quad (19)$$

which is readily rearranged to

$$-(1 + R_1 + R_0 R_1)L_1 + R_2 L_2 = W_1 \quad (20)$$

b) Plate 3: This is typical of all other interior plates of the main column and sidestrippers, where streams are neither introduced nor withdrawn. The total material balance enclosing this plate is given by

$$V_4 + L_2 - V_3 - L_3 = 0 \quad (21)$$

When Eq.(18) is used to restate the vapor flow rates V_3 and V_4 in terms of the corresponding liquid rates, the resulting equation is

$$L_2 - (1 + R_3)L_3 + R_4 L_4 = 0 \quad (22)$$

c) Plate NV: These plates are all similar in that the vapor stream from a sidestripper is returned to the plate immediately below one of them. For each plate

$$V_{NV_{i+1}} + L_{NV_{i-1}} + V_{NTOP_i} - V_{NV_i} - L_{NV_i} = 0 \quad (23)$$

and use of Eq.(18) to eliminate vapor flow rate terms gives

$$L_{NV_{i-1}} - (1 + R_{NV_i})L_{NV_i} + R_{NV_{i+1}}L_{NV_{i+1}} = -R_{NTOP_i}L_{NTOP_i} \quad (24)$$

d) Plate NW and NP: The interior plates NW and NP have in common the withdrawal of a liquid sidestream from the liquid stream leaving these plates. Eq.(18) permits the total material balance for each NW_i plate

$$V_{NW_{i+1}} + L_{NW_{i-1}} - V_{NW_i} - L_{NW_i} - W_{i+1} = 0 \quad (25)$$

to be restated as follows:

$$L_{NW_{i-1}} - (1 + R_{NW_i})L_{NW_i} + R_{NW_{i+1}}L_{NW_{i+1}} = W_{i+1} \quad (26)$$

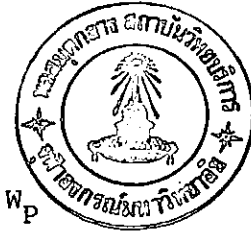
Note that L_{NW_i} represents the liquid flow rate at which the liquid stream enters plate NW_{i+1} and $(L_{NW_i} + W_{i+1})$ is the rate at which the liquid stream leaves plate NW_i .

For each NP_i plate, the total material balance will be obtained by substituting NW_i and W_{i+1} in Eqs.25 and 26 with NP_i and W_p , respectively.

e) Plate NQ: The liquid-pumparound stream W_p is returned to plate NQ_i and the balance for this plate, namely,

$$V_{NQ_{i+1}} + L_{NQ_{i-1}} + W_p - V_{NQ_i} - L_{NQ_i} = 0 \quad (27)$$

has the following form when stated in terms of the liquid flow rates,



$$L_{NO_i-1} - (1 + R_{NO_i})L_{NO_i} + R_{NO_i+1}L_{NO_i+1} = -W_P \quad (28)$$

The right-hand sides of Eqs.24 and 26 are not directly known but are simple to find by sequential direct substitution in the total material balance equations of each sidestripper. The reason is that the L_{NBOT} and FS are specified, and that normally a sidestripper linked to the main column can be simulated accurately using only two theoretical plates (64).

Thus the complete set of total material balances may be represented by a matrix equation of the form

$$T \cdot L = -F \quad (29)$$

and matrix T is a $NT \times NT$ tridiagonal matrix which is easy to solve.

The column vector F is

$$F = [f_1 \ f_2 \ \dots \ f_{NT}]^T \quad (30)$$

and contains the feed and withdrawal rates. Similarly the column vector L is

$$L = [L_1 \ L_2 \ \dots \ L_{NT}]^T \quad (31)$$

and contains the total flow rates of the liquid.

4.2.3 Component Material Balances

The component material balances may be stated in terms of either the vapor or the liquid flow rates by use of the equilibrium relationships. The presence of two perfectly immiscible liquid

phases on the first stage and the typical two-phase (vapor and liquid) behavior on all subsequent stages call for a special treatment of water on stages 1 and 2. Development of the component material balances for all components, except water, are developed for the first and second stages, and then water balances on these two stages are developed.

The equilibrium relationship is used to state the component material balances in terms of the vapor flow rates. Starting with the equilibrium relationship

$$y_{ji} = K_{ji} x_{ji} \quad (32)$$

where i is any component and j is any plate, the mole fractions in Eq.(32) may be stated in terms of the component flow rate of the vapor and the absorption factors by making of the defining relationships $v_{ji} = V_j y_{ji}$ and $l_{ji} = L_j x_{ji}$ as follows:

$$v_{ji} = (K_{ji} V_j / L_j) l_{ji} = (\theta_j K_{ji}) (V_j / L_j) l_{ji} \quad (33)$$

or

$$l_{ji} = A_{ji} v_{ji} \quad (34)$$

Here the absorption factor A_{ji} is defined as

$$A_{ji} = (1 / \theta_j K_{ji}) (L_j / V_j) \quad (35)$$

Then, the component material balance for any simple plate j

$$v_{j+1,i} + l_{j-1,i} - v_{ji} - l_{ji} = 0 \quad (36)$$

may be stated in terms of the vapor flow rate by use of Eq.(34) as follows:

$$A_{j-1,i} v_{j-1,i} - (1 + A_{ji}) v_{ji} + v_{j+1,i} = 0 \quad (37)$$

In accordance with the model assumed for plates 1 and 2, the component material balance for these two plates are formulated as follows. If water is denoted as component c, then, the component material balance on plate 1 for any component other than water is given by

$$v_{2i} - v_{1i} - l_{1i} - w_{1i} = 0 \quad (i \neq c) \quad (38)$$

Since both liquid streams leaving the condenser have the same composition, therefore

$$w_{1i} = (W_1/L_1) l_{1i} \quad (i \neq c) \quad (39)$$

Using this condition and the equilibrium relationship given in Eq.(34), the component-material balance can be stated as

$$- [1 + A_{1i} + (W_1/L_1) A_{1i}] v_{1i} + v_{2i} = 0 \quad (i \neq c) \quad (40)$$

By a similar procedure, the component material balance for the second stage

$$v_{3i} + l_{1i} - v_{2i} - l_{2i} = 0 \quad (i \neq c) \quad (41)$$

can be stated as

$$A_{1i}v_{1i} - (1+A_{2i})v_{2i} + v_{3i} = 0 \quad (i \neq c) \quad (42)$$

The component material balances for the remaining stages are developed in an analogous manner, and the complete set of equations so obtained may be stated in matrix form as follows

$$C_i \cdot v_i = -f_i \quad (i \neq c) \quad (43)$$

where

$$v_i = [v_{1i} \ v_{2i} \ \dots \ v_{N,i}]^T$$

$$f_i = [0 \ \dots \ 0 \ v_{Fi} \ l_{Fi} \ 0 \ \dots \ 0]^T$$

The $N \times N$ square matrix C_i differs from a tridiagonal matrix in the appearance of only four nonzero elements to the right and four nonzero elements to the left of the tridiagonal band of elements. The four nonzero elements to the right of the tridiagonal band result from the return of the vapor streams from the sidestrippers, and the four elements to the left of the tridiagonal band result from the introduction of the sidestreams W_2 , W_3 , W_4 , and W_5 to the sidestrippers. The hydrocarbon feed F enters on plate NF , and v_{Fi} is in row $NF-1$ while l_{Fi} is in row NF .

4.2.4 Component Material Balances for Water

Since the two liquid phases (the water phase and the hydrocarbon phase) in the accumulator are taken to be immiscible, it follows that

$$w_{0c} = w_0 \quad (44)$$

$$l_{1c} = 0 \quad (45)$$

Thus the component material balance for water on plate 1 (the condenser-accumulator section) is given by

$$v_{2c} - v_{1c} - w_{0c} = 0 \quad (46)$$

Since the partial pressure of water vapor above the two liquid phases in the accumulator is equal to its vapor pressure, it is evident that

$$P_{1c} = p_{1c} = (v_{1c}/V_1)P \quad (47)$$

where P_{1c} is the vapor pressure of water at the temperature T_1 of the accumulator and p_{1c} is the partial pressure of water in the accumulator. Symmetry of the equations is preserved by restating the flow rate of water w_{0c} in terms of the vapor flow rate v_{1c} . Commencing with

$$w_{0c} = W_0 = (W_0/v_{1c})v_{1c} \quad (48)$$

and making use of Eq.(47) gives

$$w_{0c} = W_0 v_{1c} / [V_1 (P_{1c}/P)] = A_{0c} v_{1c} \quad (49)$$

Use of this relationship permits the water balance on first stage to be restated as follows

$$- (1 + A_{0c})v_{1c} + v_{2c} = 0 \quad (50)$$

For plate 2, the water balance is

$$v_{3c} - v_{2c} - l_{2c} = 0 \quad (51)$$

since $l_{1c} = 0$. For plates 2 through N, water is taken to be a two-phase component and the equilibrium relationship given by Eq.(34) may be used to restate the water balance on the second stage as follows:

$$- (1 + A_{2c})v_{2c} + v_{3c} = 0 \quad (52)$$

4.2.5 Corresponding Set of Independent Functions

For the general case of plate j , in which a single liquid phase is in equilibrium with the vapor phase, there exist two independent variables, namely, θ_j (or Q_C or Q_R) and T_j . The total number of $2N+1$ independent variables for the topping column results from the existence of two immiscible liquid phases in the accumulator, which gives rise to three independent variables [θ_0, θ_1 (or Q_C), T_1] for plate 1.

In order to solve for the $2N+1$ independent variables via the Newton-Raphson method, $2N+1$ independent equations must be selected and expressed in functional form. The equations so selected are the $N+1$ equilibrium relationships and the N enthalpy balances.

The $N-1$ equilibrium functional expressions for stages 2 through N are formulated by commencing with the condition that a set of the independent variables is to be found such that $F_j = 0$ for all j ($j = 2, 3, \dots, N$). Here

$$F_j = \left(\sum_{i=1}^c l_{ji} \right) / L_j - \left(\sum_{i=1}^c v_{ji} \right) / V_j \quad (53)$$

The equilibrium relationship given by Eq.(34) may be used to reduce Eq.(53) to either a bubble point or dew point function. The dew point form of the function is obtained by eliminating the l_{ji} 's to give

$$F_j = (1/V_j) \sum_{i=1}^c [(1/K_{ji}) - 1] v_{ji} \quad (54)$$

The existence of two liquid phases on stage 1 leads to two independent equilibrium functional expressions. The functional expression for the hydrocarbon phase is obtained by using Eq.(53) and the fact that $l_{1c} = 0$. Thus

$$F_1 = (1/V_1) \sum_{i=1}^c [(1/K_{ji}) - 1] v_{1i} - v_{1c} \quad (55)$$

The functional form of the equilibrium expression for the liquid-water phase on plate 1 is obtained by using the equilibrium relationships in Eq.(47). Rearrangement of this equation gives

$$F_0 = [v_{1c}/V_1 (P_{1c}/P)] - 1 \quad (56)$$

The enthalpy balance equations are formulated for any stage j in a manner analogous to that demonstrated for an interior stage j such as stage $j=3$. The enthalpy balance enclosing stage j may be stated in the following form:

$$\sum_{i=1}^c [v_{j+1,i} H_{j+1,i} + l_{j-1,i} h_{j-1,i} - v_{ji} H_{ji} - l_{ji} h_{ji}] = 0 \quad (57)$$

Elimination of l_{ji} by use of the component material balance

$$v_{j+1,i} + l_{j-1,i} - v_{ji} - l_{ji} = 0 \quad (58)$$

for stage j followed by the restatement of the expression in functional notation yields

$$G_j = \sum_{i=1}^C [v_{j+1,i}(H_{j+1,i} - h_{ji}) + l_{j-1,i}(h_{j-1,i} - h_{ji}) - v_{ji}(H_{ji} - h_{ji})] \quad (59)$$

The normalized form of the enthalpy balance equation for any stage j may be expressed as

$$G_j = G_{uj}/G_{lj} \quad (60)$$

$$\begin{aligned} \text{where } G_{uj} = & \sum_{i=1}^C [C_{1j}v_{j+1,i}(H_{j+1,i} - h_{ji}) + C_{2j}l_{j-1,i}(h_{j-1,i} - h_{ji}) \\ & + C_{3j}v_{Pi}(H_{Pi} - h_{ji}) + C_{4j}l_{Pi}(h_{Pi} - h_{ji}) + C_{5j}v_{Fi}(H_{Fi} - h_{ji}) \\ & + C_{6j}l_{Fi}(h_{Fi} - h_{ji})] \quad 1 \leq j \leq N \quad (61) \end{aligned}$$

$$G_{lj} = \sum_{i=1}^C v_{ji}(H_{ji} - h_{ji}) + C_{7j}Q_j \quad 1 \leq j \leq N \quad (62)$$

The heat duty for plate j is denoted by Q_j . The subscripts P and F refer to a pumparound stream and an external feed stream, respectively.

In summary, a total of $N+1$ equilibrium equations (F_0, F_1, \dots, F_N) and N enthalpy balance equations (G_1, G_2, \dots, G_N) constitute a system of $2N+1$ simultaneous nonlinear equations in the $2N+1$ independent variables ($\theta_0, \theta_1, \dots, \theta_N, T_1, T_2, \dots, T_N$).

4.2.6 Algorithm for Independent Function Evaluation

From the above presentation, evaluation of the independent functions may be carried out sequentially as follows:

Step 1: Based upon the assumed values of $(V_j/L_j)_a$ and the latest iterative values of θ_j , solve Eq.(29) for the values of L_j , and then find V_j via Eq.(18).

Step 2: For $i=1$ use the latest iterative values of T_j and θ_j to find K_{ji} , then A_{ji} ($j=1,2,\dots,N$), respectively. Next solve Eq. (43) for v_{ji} . By repeating the same procedure for $i=2,3,\dots,c$, find all the v_{ji} , l_{ji} corresponding to the latest iterative values of θ_j and T_j .

Step 3: Evaluate the equilibrium functions via Eq.(54-56) using the values obtained in step 2.

Step 4: Find H_{ji} and h_{ji} from T_j and then evaluate the enthalpy functions via Eq.(60-62).

Thus the $2N+1$ independent functions $f(x)$ can be evaluated from the $2N+1$ independent variable x .

ศูนย์วิทยทรัพยากร
จุฬาลงกรณ์มหาวิทยาลัย